Impact of water activity on microbial growth in bentonite clay

by

Rhiannon Punch

A thesis
presented to the University of Waterloo
in fulfillment of the
thesis requirement for the degree of
Master of Science
in
Biology

Waterloo, Ontario, Canada, 2023

© Rhiannon Punch 2023

Author's Declaration

This thesis consists of material all of which I authored or co-authored: see Statement of Contributions included in the thesis. This is a true copy of the thesis, including any required final revisions, as accepted by my examiners. I understand that my thesis may be made electronically available to the public.

Statement of Contributions

Chapter 2

Katja Engel and Emilie Spasov cultivated aerobic and anaerobic heterotrophs, as well as SRB from single replicates of anoxic microcosms hydrated with water or SRB medium at low, medium, and high water activities at the one-week timepoint. Rachel Beaver assisted with PCR, library preparations, and high-throughput sequencing of all samples included in this research.

Abstract

Canada is in the process of designing and implementing a deep geological repository (DGR) for long-term storage of used nuclear fuel. This proposed storage structure will be a multi-barrier system placed 500-800 metres belowground at a stable and informed host site within either a crystalline or sedimentary rock bed. Bentonite clay, which swells upon saturation, will be used to encase copper-coated used fuel containers and seal the DGR. The presence of naturally occurring microorganisms in the bentonite or subsurface environment, specifically anaerobic sulfate-reducing bacteria (SRB), is an important design consideration in the DGR due to their potential metabolic production of copper-corroding sulfides. For this reason, it is essential to study conditions for bentonite clay that will suppress microbial activity. Using pressure vessels for saturation, previous studies demonstrate that microbial growth is suppressed in compacted bentonite at swelling pressures over 2 MPa and water activities of 0.96 or less. After DGR establishment, the system will experience drying as radioactive heat dissipates, followed by a period of cooling and resaturation. Additionally, the salinity of groundwater penetrating the bentonite will vary depending on the chosen host rock. It is therefore important to investigate microbial responses to a variety of conditions in bentonite to account for possible combinations that will occur in the DGR and identify thresholds that suppress microbial proliferation. My thesis research explored the effects of water activity on Wyoming MX-80 bentonite clay in relation to microbial viability, abundance, and community composition, without the influence of pressure, by assessing microcosm samples in combinations of conditions using water activity, hydration solution, and oxygen presence.

Microbial abundance estimates correlated with increasing water activity in oxic conditions. Highest overall microbial abundances were observed for oxic microcosms hydrated with SRB medium. Estimates for SRB remained unchanged for all conditions. No significant microbial proliferation occurred in microcosms hydrated with high-salinity medium or anoxic microcosms. These results suggest higher microbial abundances in the presence of high water activities and nutrient availability, and demonstrate suppression of microbial growth associated with both high-salinity hydration and anoxic incubation conditions.

Microbial community profiles based on amplicon sequence variants resulting from direct 16S rRNA gene sequencing of oxic microcosms hydrated with water, low-salinity medium, or SRB medium revealed a dominance of *Actinobacteriota*, specifically ASVs affiliated with *Saccharopolyspora* in low and medium water activities and *Streptomyces* in medium and high water activities. These results indicate a growth dependence of specific actinobacterial taxa based on water activity. There were no consistent community composition pattern changes for anoxic microcosms or microcosms hydrated with high-salinity medium, consistent with a lack of growth based on cultivation-based and qPCR-based approaches.

Quantification of fungal 18S rRNA genes from oxic samples hydrated with water or SRB medium revealed increasing abundances of fungi, specifically in microcosms hydrated with SRB medium. These data suggest that abundance estimates of aerobic heterotrophs from microcosms may include fungal colonies that match expected morphologies commonly observed on corresponding cultivation plates.

Studying the effects of water activity and hydration media on bentonite is essential to understanding how microbial viability will be affected by water activity within a DGR environment, even in the absence of pressure. Overall, the results demonstrate that microbial growth is slowed by relatively low water activity, and that anoxic conditions and high-salinity water further suppresses bentonite-associated microbial growth. These results inform ongoing pressure vessel experiments that combine both water activity and pressure as controlling environmental parameters and will help guide DGR design specifications and the associated safety case for implementation.

Acknowledgements

I would like to thank my supervisor, Dr. Josh Neufeld, for accepting me into his lab and always providing support, encouragement, and an enjoyable learning environment over the duration of this project. I would also like to thank my committee members, Dr. Barb Butler and Dr. Laura Hug, for their guidance and contributions to this work.

Thank you to my lab mates, for always encouraging and supporting me, helping me with bioinformatics, and for the meaningful relationships that we have established. Thank you to Rachel Beaver, for always going above and beyond to provide me with her knowledge and insight, and for her contributions to this project. Thank you to Katja Engel for her continued input into this research and depth of knowledge in this field. Thank you to Cailyn Perry, Peter Palermo, and Milena Rabu for their assistance with wet lab work.

Thank you to Dr. Simcha Stroes-Gascoyne for collaboration, knowledge about bentonite clay microbiology, and providing the original suggestion for this thesis research. Thank you to Dr. Greg Slater and Dr. Myrna Simpson for their ongoing collaboration surrounding PLFA and NOM data. I am grateful to Dr. W. Jeffrey Binns and the Nuclear Waste Management Organization, Natural Sciences and Engineering Research Council, and Ontario Research Fund for supporting and funding this project.

Thank you to family and friends for always supporting me and providing reassurance when I needed it most. Thank you for encouraging me and listening to my practice presentations, even when you had no idea what I was talking about.

My time spent in the Neufeld lab has introduced me to good friends, challenged me to be a better scientist, and better shaped my understanding of microbiology. I will forever be grateful for this experience.

Dedication

For my Papa, Thomas Francis Punch, who lived with my family for most of my life, and who passed away during the course of this project. Growing up, there was not a day where I came home from school that he didn't ask me, "Did you learn anything new today?". As a teacher, the education of his grandchildren was greatly supported, and he always made sure we had at least a little bit of fun doing it as well. This thesis exists because of the "village" of people like him who have encouraged me and provided me with the building blocks for a fruitful and knowledgeable life. This thesis represents me learning something new every day.

Table of Contents

Author's Declaration ii
Statement of Contributions iii
Abstract iv
Acknowledgements vi
Dedication vii
List of Figures x
List of Tables xiii
List of Abbreviations xiv
Chapter 1 Introduction 1
1.1 Canadian used nuclear fuel 1
1.2 The Deep Geological Repository 2
1.3 Bentonite clay 3
1.4 Evolution of the DGR environment 4
1.5 Microbiology of a DGR 6
1.5.1 Microbial activity 6
1.5.2 Sulfate reduction in the subsurface environment 7
1.5.3 Microbiologically influenced corrosion 8
1.5.4 Other subsurface metabolisms 9
1.6 Microbiological growth suppression in a DGR 11
1.7 Geochemistry and hydrogeology of the DGR 14
1.8 Current state of the field 16
1.8.1 Methods for microbiological analysis in bentonite 16
1.8.2 Recent research 17
1.9 Objectives 18
Chapter 2 Materials and methods 20
2.1 Bentonite hydration and microcosm set-up 20
2.1.1 Large-scale microcosms 21
2.2 Water activity and moisture content 21
2.3 Cultivation 22
2.3.1 Heterotrophs 22
2.3.2 Sulfate-reducing bacteria 23
2.4 DNA extraction and quantification 23

2.4.1 Microcosm bentonite samples 23
2.4.2 Cultures 24
2.5 Quantitative PCR 24
2.6 Amplification and high-throughput sequencing of the 16S rRNA gene 25
2.7 Sequence analysis 26
2.8 Quantification of fungi 27
Chapter 3 Results and discussion 28
3.1 Bentonite hydration 28
3.2 Microbial viability and abundance 31
3.3 Microbial community composition 37
3.3.1 16S rRNA gene sequencing run comparison 37
3.3.2 Microbial community composition of microcosm samples 41
3.3.3 Indicator species identified across microcosm parameters 49
3.4 Application to DGR research 54
3.5 Large-scale microcosms 55
3.6 Comparison of community profile assays 61
Chapter 4 Conclusions and future directions 68
Bibliography 72

List of Figures

Figure 1.1 Schematic of the production of CANDU nuclear fuel from uranium dioxide. 1
Figure 1.2 Conceptual diagram of the NWMO's multi-barrier design for Canada's DGR..... 3
Figure 1.3 Predicted timeline of environmental conditions in the DGR lifetime. 6
Figure 1.4 Geospheric microbiologically gas-driven cycle hypothesis. 11
Figure 1.5 Cultural aerobic heterotroph abundance (CFU/gram dry weight) as a function of water activity in Wyoming MX-80 bentonite saturated with different salinities. 13
Figure 3.1 Uniformly hydrated bentonite samples at A) low (0.93), B) medium (0.96), and C) high water activities. 28
Figure 3.2 Average water activity and moisture content measurements in each medium and target water activity..... 29
Figure 3.3 All water activity and moisture content measurements in each medium, oxygen condition, and target water activity across time..... 31
Figure 3.4 Average abundances of the 16S rRNA gene (copies/gdw), aerobic heterotrophs (CFU/gdw), anaerobic heterotrophs (CFU/gdw), and SRB (MPN/gdw) from as-received bentonite or hydrated oxic microcosms at low, medium, and high water activities over time. 32
Figure 3.5 Average abundances of the 16S rRNA gene (copies/gdw), aerobic heterotrophs (CFU/gdw), anaerobic heterotrophs (CFU/gdw), and SRB (MPN/gdw) from as-received bentonite or hydrated anoxic microcosms at low, medium, and high water activities over time. 35
Figure 3.6 PCR amplification of samples including microcosms hydrated with each medium at low (L), medium (M), or high (H) water activities from sequencing run two based on visual agarose gel electrophoresis bands 39
Figure 3.7 Boxplots with a jitter overlay displaying average read counts from 16S rRNA gene sequencing compared across all bentonite samples within A) each hydration medium, B) each water activity, C) each timepoint, and D) both oxygen conditions. 40
Figure 3.8 Principal coordinate analysis (PCoA) biplots using Bray-Curtis dissimilarity distances comparing A) water activity, B) oxygen condition, C) medium, and D) timepoint across samples..... 42

Figure 3.9 Bubble plot of the 16S rRNA gene profile of oxic microcosms across all sequenced timepoints.. 44
Figure 3.10 Bubble plot of the 16S rRNA gene profile of anoxic microcosms across all sequenced timepoints.. 48
Figure 3.11 Bubble plot of the 16S rRNA gene profiles of indicator ASVs in oxic microcosms across all sequenced timepoints as determined by an indicator species analysis 51
Figure 3.12 Relative abundances of identified indicator ASVs affiliated with *Saccharopolyspora* and *Streptomyces* compared to raw water activity measurements of all sequenced samples 53
Figure 3.13 Average water activity and moisture content measurements in small-scale and large-scale microcosms at targeted water activities 56
Figure 3.14 Average abundances of the 16S rRNA gene (copies/gdw), aerobic heterotrophs (CFU/gdw), anaerobic heterotrophs (CFU/gdw), and SRB (MPN/gdw) from large-scale or small-scale microcosms at low or high water activities over time 58
Figure 3.15 Bubble plot of the 16S rRNA gene profile of small-scale and large-scale microcosms across all timepoints 60
Figure 3.16 Principal coordinate analysis (PCoA) biplot using Bray-Curtis dissimilarity distances comparing 16S rRNA gene sequencing data of clays versus cultures derived from the clay 62
Figure 3.17 Bubble plot of the 16S rRNA gene profiles of ASVs from oxic and anoxic R2A plates inoculated from oxic microcosms hydrated with water or SRB medium up to the three-month timepoint. 63
Figure 3.18 Bubble plot of the 16S rRNA gene profiles of ASVs from SRB medium inoculated from oxic microcosms hydrated with water or SRB medium up to the three-month timepoint. 64
Figure 3.19 Images of oxic R2A plates derived from oxic microcosms hydrated with SRB medium to an A) medium water activity or a B) high water activity cultivated at the three-month timepoint as examples of the presence of large, fuzzy, dark green colonies and small, white, punctiform colonies..... 65

Figure 3.20 Average abundance of the 18S rRNA gene (copies/gdw), from oxic microcosm samples hydrated with water or SRB medium up to the three-month timepoint to determine the potential presence of fungi. 67

List of Tables

Table 1.1 Major ionic composition of reference groundwaters for potential DGR host sites. 15
Table 2.1 Volumes of water necessary to achieve specific water activities in a fixed mass of bentonite 20
Table 3.1 Indicator ASVs and strength associations as determined by an indicator species analysis for all media and water activities in hydrated oxic microcosms 50

List of Abbreviations

APM	Adaptive phased management
ASV	Amplicon sequence variant
ATP	Adenosine triphosphate
a_w	Water activity
BSA	Bovine serum albumin
Ca	Calcium
CANDU	Canadian Deuterium Uranium
CFU	Colony forming unit
Cl	Chlorine
DGR	Deep geological repository
Fe	Iron
Fe^{2+}	Iron(II)
Fe^{3+}	Iron(III)
g/L	grams per litre
gdw	gram dry weight
HCB	Highly compacted bentonite
HCO_3^-	Bicarbonate
H_2S/HS^-	Hydrogen sulfide/bisulfide
K	Potassium
MC	Moisture content
Mg	Magnesium
MIC	Microbiologically influenced corrosion
MPN	Most probable number
Na	Sodium
NaCl	Sodium chloride
NFWA	Nuclear Fuel Waste Act
NOM	Natural organic matter
NTC	No template control
NWMO	Nuclear Waste Management Organization
PBS	Phosphate buffered saline

PCoA	Principal coordinate analysis
PCR	Polymerase chain reaction
PLFA	Phospholipid fatty acid
PMA	Propidium monoazide
qPCR	Quantitative polymerase chain reaction
R^2	Coefficient of determination
R2A	Reasoner's 2 Agar
SO_4^{2-}	Sulfate
SRB	Sulfate-reducing bacteria
TDS	Total dissolved solids
UFC	Used fuel container
UO_2	Uranium dioxide

Chapter 1

Introduction

1.1 Canadian used nuclear fuel

Nuclear power provides an emission-free energy alternative to fossil fuels. In Canada, nuclear energy is processed by power generators called CANDU (CANada Deuterium Uranium) reactors [1]. To produce fuel for CANDU reactors, uranium dioxide (UO_2) derived from natural uranium ore is pressed and baked into ceramic pellets [1]. These pellets are then stacked in zirconium-tin alloy tubes to form fuel pencils, which are welded together to create fuel bundles that are used directly for energy generation (Figure 1.1) [1].

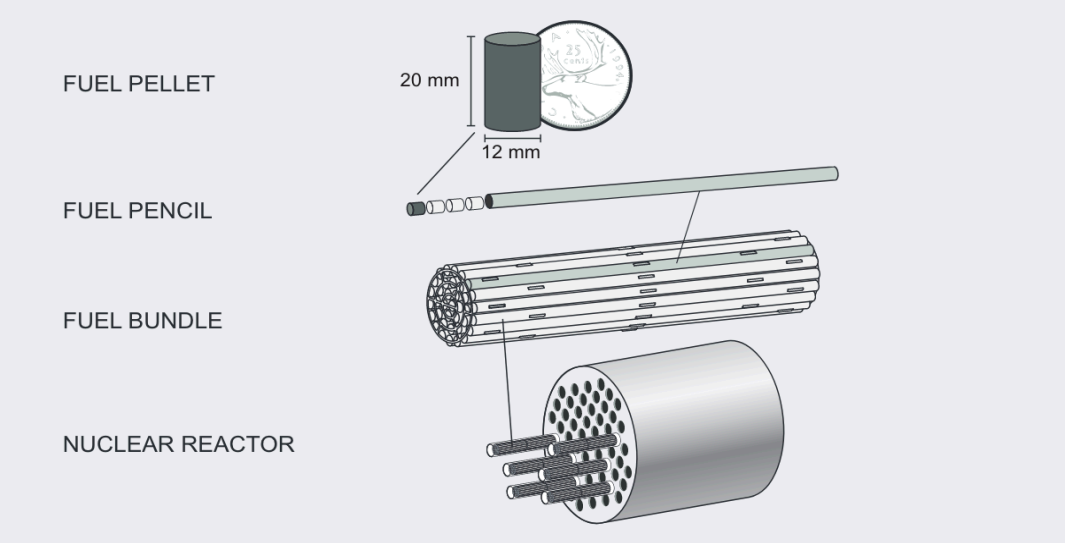


Figure 1.1. Schematic of the production of CANDU nuclear fuel from uranium dioxide. Adapted from [1].

Once this fuel is spent, the waste will remain radioactive and exceed the radioactivity levels of natural uranium for approximately one million years [1]. Currently, around three million used nuclear fuel bundles are stored at or near reactor sites in Canada, first in pools of water for cooling, then followed by dry storage containers [1]. This number is projected to increase to 5.5 million by the end of reactor lifetimes. Continued use of nuclear energy drives the need for a sustainable, safe, and long-term storage solution for used nuclear fuel, especially if nuclear energy production is favoured in attempts to achieve a future of net-zero emissions.

In 2002, the Nuclear Waste Management Organization (NWMO) was established in Canada under the Nuclear Fuel Waste Act (NWFA) to recommend, design, and implement a solution for used nuclear fuel, leading to selection of the Adaptive phased management (APM) approach [2]. This plan bridges technical methods of transportation, isolation, and storage of used nuclear fuel with a management system that allows for an open and transparent process that involves communities. The technical objective of APM is containment of used nuclear fuel in a deep geological repository (DGR), which is designed to be a multi-barrier system 500-800 metres belowground at a stable geological site and a willing and informed host community [1, 3].

1.2 Deep Geological Repository

The proposed DGR system will consist of five barriers to isolate radioactive used nuclear fuel (Figure 1.2). Each barrier provides independent protection to accommodate any potential failure in a previous barrier [3]. First, ceramic fuel pellets deliver a level of protection due to their durable nature, providing resistance against high temperatures, water, and erosion [3, 4]. Second, zirconium-tin alloy ("Zircaloy") fuel pencils offer corrosion-resistant isolation of fuel pellets [1, 3]. Third, bundles will be placed within corrosion-resistant copper-coated used fuel containers (UFCs) made of carbon steel for durability. The UFC body and lid will be welded together to contain 48 fuel bundles in a carbon steel pipe [3, 5]. The UFCs are designed to contain radionuclides until radioactive decay to a safe level, hence their ability to withstand external pressures from surrounding geology as well as potential glaciation in future ice ages [3, 4]. Fourth, buffer boxes surrounding the UFCs will consist of highly compacted bentonite (HCB) clay [3]. Due to the natural swelling characteristics of this montmorillonite-rich clay upon saturation, radionuclides will be insulated even in the event that they are released from a UFC. Buffer boxes will be stacked two high and placed in large emplacement rooms within the DGR [6]. All surrounding spaces will be backfilled with pelleted bentonite called gapfill material (GFM) [5, 6]. Fifth, after closure of the DGR, groundwater from the surrounding geosphere consisting of a crystalline or sedimentary rock formation will saturate the bentonite to form a pressured seal [3, 6]. This host rock formation will act as the final stable barrier for radionuclide isolation [3].

The concept of a DGR for the stable and long-term storage of used nuclear fuel is also being anticipated in countries such as Finland, France, Japan, Sweden, Switzerland, and the United Kingdom [4]. Collaboration with other nations and studying natural analogues allows knowledge dissemination as well as safety assessments for the construction of a Canadian DGR. The Cigar Lake uranium deposit in Saskatchewan, Canada, provides a natural example of the containment of radioactive uranium by surrounding clay in the subsurface and supports the proposal that a DGR can exist and isolate radionuclides for millions of years [3, 5, 7, 8].

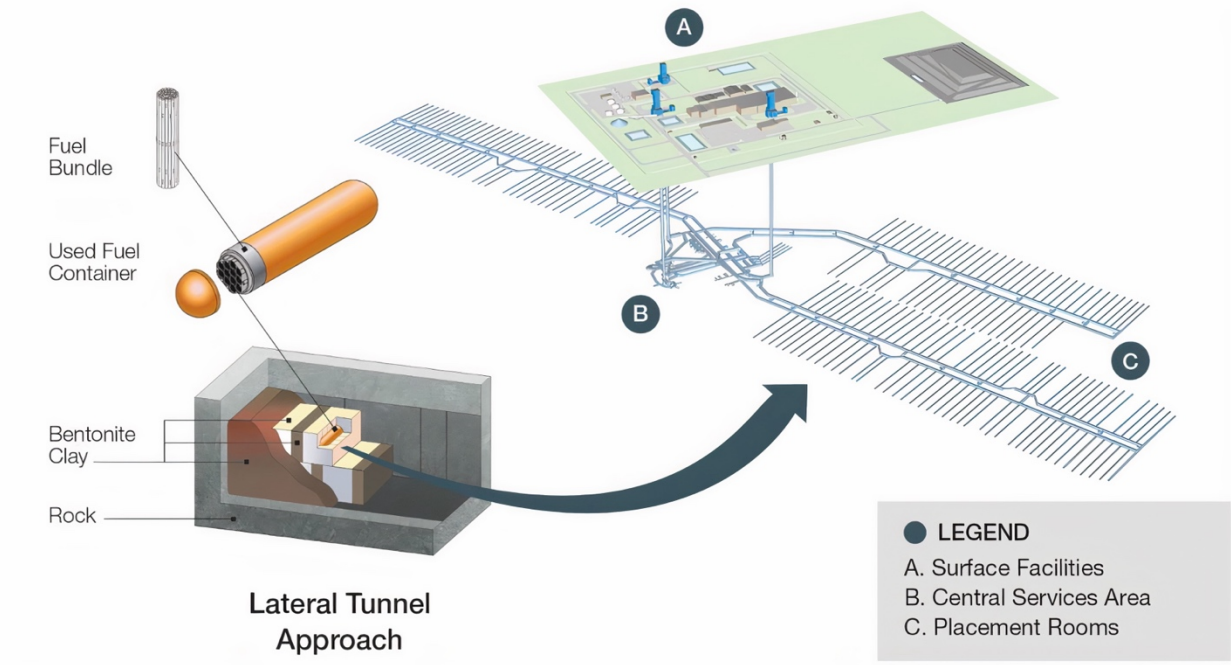


Figure 1.2. Conceptual diagram of the NWMO's multi-barrier design for Canada's DGR [5]. Lighter coloured bentonite clay represents the buffer boxes; darker coloured clay is gapfill material.

1.3 Bentonite clay

Bentonite clay is a powerful sealant due to its natural swelling capacity when saturated and has been considered for use as a buffer material in used nuclear fuel repositories for over 40 years [3, 9]. Depending on individual repository design specifications, including host rock and groundwater compositions, there are several types of

bentonites that countries are investigating as a buffer material for used nuclear fuel. These include bentonites dominated by sodium, calcium, iron, or quartz; clay composition affects swelling capacities, grain sizes, and sealing properties [9, 10]. Wyoming MX-80 bentonite clay has been chosen by Canada as the reference bentonite to be used in a DGR. Specifically, MX-80 is a sodium bentonite with a particle size of 80 mesh, or 0.177 mm [9, 10]. This material was formed approximately 100 million years ago in deposits under current Wyoming, USA, from ancient volcanic ash that was transformed into montmorillonite-rich clay shale [3, 5, 10]. Montmorillonite is a swelling mineral in the smectite group that comprises the majority of MX-80 bentonite [9, 10]. Montmorillonite consists of net negatively charged layers that take up ions and water through three interactions: interlayer-water, absorbed water on the outside surface, and free water between particles, ultimately causing the material to swell [9–11].

Exposed to temperatures exceeding 140°C, MX-80 bentonite can be converted into a non-swelling mineral called illite [5, 6, 10]. For this reason, the HCB buffer boxes (1 m x 1 m x 2.8 m) will be separated by 1.5-1.7 m spacing to prevent UFCs from reaching temperatures over 100°C as radioactive heat is generated [6]. A suitable buffer must have sufficient thermal conductivity to prevent localization of high temperatures while also achieving a low hydraulic conductivity for the prevention of material migration [10, 12]. High total dissolved solids (TDS) content within the bentonite or in the surrounding saturating groundwaters can affect the swelling capacity of bentonite [10]. To counteract this effect, an increased dry density of bentonite in the DGR will achieve a high swelling pressure and low pore space [5, 10]. To act as a suitable buffer box encasing UFCs and isolating radionuclides in the event of release, the NWMO has established that HCB will be used at an average dry density over 1600 kg/m^3 and a moisture content around 20% [5, 10]. To backfill void spaces, GFM consisting of granulated MX-80 bentonite will be used at a moisture content between 2-3% and a dry density around 1400 kg/m^3.

1.4 Evolution of the DGR environment

During its initial lifetime after being sealed, the DGR will experience stages of variability before reaching a state of equilibrium (Figure 1.3). During the first stage,

radioactive heat will dissipate from the UFCs, generating high temperatures and drying of the HCB buffer boxes and surrounding backfill area, causing clay shrinkage and ultimately decreasing swelling pressure [13]. It is predicted that the DGR will reach a temperature over 80°C after approximately 10 years [14, 15]. This increase in temperature will cause both liquid and gaseous phases of water to be present in the buffer material [15]. A heat-associated reduction in saturation will decrease pore connectivity, slowing dispersal of dissolved species (unless diffusing through a gaseous phase) [16]. Such conditions are expected to help minimize UFC surface corrosion.

During the second stage of a DGR lifetime, as temperatures stabilize over time, the system will resaturate as water returns, resulting in further changes in dry density and swelling pressure of the buffer material [13]. The system is expected to cool to ambient temperatures comparable to the host rock (approximately 10-20°C) over 10,000 years [14, 15]. During this phase, the DGR environment will deplete residual oxygen and become anoxic. Although a DGR will initially contain atmospheric oxygen that is trapped in orifices and pores of the bentonite [5], oxygen will be depleted by corrosion, adsorption, oxidation of minerals, and microbial processes [5, 15]. Although there is no specific threshold to determine an anoxic state, a previous Canadian reactive-transport model suggested that the initial oxygen concentration in the DGR will be reduced by five orders of magnitude 57 years after closure, and by nine orders of magnitude after 200 years, and an indefinite anoxic state will be reached at some point between these time frames [14, 15]. Other models have found that anoxic conditions might establish as soon as a few weeks to months after repository closure [14, 17]. Before oxygen depletion, intercalation of groundwaters back into the system during the cooling phase might allow the movement of dissolved species and oxidizing agents to reach UFC surfaces, causing potential localized corrosion [16]. Once anoxic conditions are established by the consumption of oxygen, the governing source of potential UFC corrosion will be any microbial metabolic activity that produces bisulfide (HS^-), which can react directly with the copper-coating of the UFC [14, 16].

Eventually, the DGR system will reach a state of equilibrium where there is homogeneity in saturation and corresponding dry density and swelling pressure [13]. Because

saturation is dependent on the hydraulic activity of the host rock, it is predicted that the system will reach full saturation at approximately 50 years for a crystalline rock host, or 5,000 years for a sedimentary rock host [16]. Before this point, the DGR will experience variability and gradients of temperature, pressure, dry density, and oxygen presence.

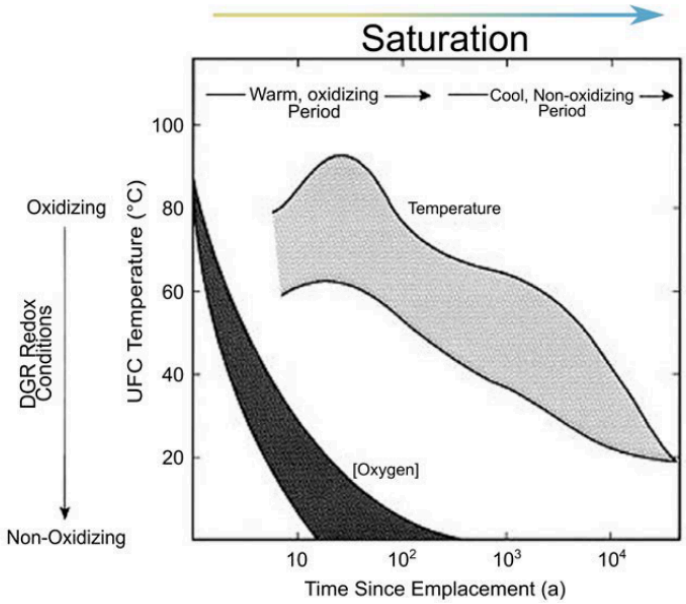


Figure 1.3. Predicted timeline of environmental conditions in the DGR lifetime. Time frames to reach full saturation will depend on the hydraulic conductivity of the host rock. Image from a previous publication [14] and further adapted from a previous publication [15].

1.5 Microbiology of a DGR

1.5.1 Microbial activity

Within a proposed DGR environment, a diverse community of microorganisms could be introduced during repository construction, from bentonite, and infiltration of naturally occurring microorganisms from surrounding groundwaters and host rock [5, 18, 19]. Although the DGR will represent an "extreme" environment for most microbial life (e.g., high temperatures, pressures, saline groundwaters, low nutrient content), it is important to study how microbial activity might affect DGR barrier stability should conditions become favourable for germination of spore formers and proliferation of desiccation-resistant bacteria

[5, 13, 20]. In the UFCs, there will be little availability of nutrients and water, as well as exposure to radionuclides and heat [5]. For these reasons, microbial activity is not expected to pose a threat to UFC stability and may even cause biomineralization of UO_2 in reducing conditions [5, 21–23]. However, cultivation from MX-80 bentonite buffer material has revealed the presence of aerobic and anaerobic heterotrophs, as well as anaerobic sulfate-reducing bacteria (SRB), including the genera *Bacillus, Pseudomonas, Desulfosporosinus*, and *Desulfovibrio* [5, 13, 18–20, 24]. In addition, microbial communities that naturally occur in subsurface environments, although usually low in biomass, may be present in sites selected to host the DGR [25].

1.5.2 Sulfate reduction in the subsurface environment

Once anoxic conditions are established in the DGR, the activity of SRB is a concern due to the potential for naturally occurring sulfates being reduced into copper-corroding sulfides that could contribute to microbiologically influenced corrosion (MIC) [5, 13]. Sulfate-reducing metabolisms play a key role in the sulfur cycle and have been found in a range of environments, including soil, wastewater, groundwater, the deep subsurface, and bentonite clay [5, 20, 24, 26–28]. In addition, SRB can tolerate a range of these environments, having been detected at extreme pH levels, temperatures, and salt concentrations [26, 27]. Mesophilic SRB are common, with some species, such as *Desulfovibrio thermophilus*, exhibiting thermophilic growth [29]. Certain SRB, like *Desulfotomaculum*, can form spores and are resistant to desiccation [30]. Concentrations of naturally occurring sulfates exist in bentonite clay as well as surrounding host rock and groundwater environments. These sulfates are usually present at low concentrations; however, certain host rocks may maintain higher concentrations than others [5, 14, 31, 32]. For these reasons, SRB may be prevalent in subsurface and bentonite environments and can potentially survive in DGR-like conditions. Both autotrophic and heterotrophic metabolisms have been observed for SRB. Autotrophic sulfate reducers use sulfate as a terminal electron acceptor coupled with hydrogen oxidation in a dissimilatory pathway to produce hydrogen sulfide (Equation 1.1), using carbon dioxide as a carbon source [5, 14, 29, 33]. This is a common pathway seen in species of *Desulfonema* and *Desulfococcus*, for example [29]. Some heterotrophic SRB are able to reduce sulfate through the incomplete oxidation of

lactate into acetate (Equation 1.2), as reported for certain *Desulfovibrio* and *Desulfotomaculum* species, whereas others can use the complete oxidation of acetate (Equation 1.3) or lactate (Equation 1.4) into carbon dioxide, such as *Desulfobacter* species [27, 29, 33, 34].

Equation 1.1: $4H_2 + SO_4^{2-} \rightarrow HS^- + 4H_2O$

Equation 1.2: $2C_3H_5O_3^- + SO_4^{2-} \rightarrow 2C_2H_3O_2^- + 2HCO_3^- + HS^- + H^+$

Equation 1.3: $C_2H_3O_2^- + SO_4^{2-} \rightarrow HS^- + 2HCO_3^-$

Equation 1.4: $2C_3H_5O_3^- + 3SO_4^{2-} \rightarrow 6HCO_3^- + 3HS^- + H^+$

Desulfovibrio africanus, a Gram-negative, anaerobic, non-spore forming heterotroph was previously cultivated as an indigenous species from Wyoming MX-80 bentonite [35]. This specific study determined that these SRB were still able to proliferate after incubation in bentonite that was previously heated to 100°C and could grow in incubations up to 40°C and salt concentrations up to 4% [35]. This evidence suggests that SRB found within MX-80 bentonite clay can survive in desiccated states and may increase in abundance should DGR conditions become favourable, despite initial heat, low water content, and saline groundwaters.

1.5.3 Microbiologically influenced corrosion

The presence of SRB in the DGR environment is of specific concern due to the metabolic production of bisulfide or hydrogen sulfide, which can then interact with the outer copper coating of the UFCs to form a copper sulfide corrosion product once anoxic repository conditions are met (Equation 1.5) [5, 14]. Although copper is naturally corrosion-resistant, it can still be susceptible to MIC [36].

Equation 1.5: $2Cu + HS^- + H^+ \rightarrow Cu_2S + H_2$

Copper corrosion caused by metabolically produced sulfides from SRB has previously been seen in estuarine environments, sulfide-contaminated seawater, and potable water systems [37]. Copper materials are specifically known to be susceptible to MIC caused

by biofilm formation on the metal surfaces [38]. However, due to initial high temperatures on UFC surfaces from heat dissipation, low water activity, low nutrient content, and the presence of gamma radiation, it is estimated that biofilm formation may not take place near UFCs for at least 10,000 years [14, 38]. Still, this possibility does not eliminate the potential for MIC to occur after these conditions, as well as in more favourable environments existing further away from UFCs, such as less-compacted bentonite or material interfaces where bentonite has not fully swelled to contact adjacent surfaces [5, 14, 38]. For example, microorganisms have been cultivated at interfaces between buffer material and host rock [39, 40]. If sulfides are present or become present at these locations and areas of high permeability and hydraulic conductivity occur during DGR resaturation, porewater could introduce these compounds further into the system, or they may become present by diffusive transport [14, 36, 38, 41].

1.5.4 Other subsurface metabolisms

In addition to SRB, microbial groups relevant for a DGR include aerobic and anaerobic heterotrophs (e.g., fermenters), denitrifying bacteria, iron-reducing bacteria, and methanogens that could be present in bentonite or the surrounding DGR environment and may deplete and produce various gases and other compounds [14, 24, 28, 32, 41, 42]. In bentonite, there is limited organic material (0.11% organic carbon in MX-80), which is an important reason why this material is usually considered low in biomass [5, 30]. However, autotrophic microorganisms are present in deep subsurface ecosystems, and hydrogen and carbon dioxide in the geosphere can provide electrons/energy and carbon sources for hydrogenotrophic bacteria and other autotrophs [28, 41]. Hydrogen has been detected in deep igneous aquifers and can be generated by multiple processes in these environments, such as the decomposition of methane to carbon and hydrogen, radioactive isotopes generating the radiolysis of water, MIC, and the reaction between carbon dioxide, methane, and water in vapours [28, 41, 43]. The presence of hydrogen and carbon dioxide can support autotrophic methanogens, such as *Methanobacterium alcaliphilum*, previously found based on 16S rRNA gene analyses in Boom clay, a material being considered for nuclear waste storage in Belgium [42, 44], and acetogenic bacteria, producing methane and acetate for further heterotrophic metabolisms, such as iron and sulfate reduction (Figure 1.4) [28, 41, 42].

Nitrogen-containing deposits and nitrates in groundwaters and host rock, or in leachate from external sources, can also provide electron acceptors for denitrifying bacteria that have been found in clay, such as certain *Pseudomonas* and *Thiobacillus* species [24, 32, 41, 42]. Denitrifying activity can cause an accumulation of nitrogen gas that can be further be used as a source of nitrogen in the subsurface or can cause fissures in the bentonite barriers [24, 41, 42]. Additionally, iron-reducing bacteria, which have also been detected in MX-80 bentonite, can reduce structural iron in bentonite from acetate or lactate oxidation [40–42, 45]. This can result in structural Fe^{3+} to Fe^{2+} transformation in bentonite, which could alter swelling capacities and hydraulic conductivity [40, 45]. For example, certain species of *Bacillus* are capable of iron reduction and have been detected based on 16S rRNA gene analyses in MX-80 bentonite that was heated to 70°C and, therefore, may survive in bentonite as spores [40].

As described previously, the DGR will not be a sterile environment and could potentially contain a diverse group of microorganisms and metabolisms, either naturally present in DGR barriers, introduced during DGR construction, or that have infiltrated from surrounding subsurface environments and groundwaters. Therefore, a self-sustaining microbial ecosystem can exist in this subterranean environment if conditions favour microbial viability and activity. Metabolites from naturally occurring bacteria and deposited organic carbon may disseminate through buffer material or be available at material interfaces for microbial activity if the DGR environment achieves high hydraulic conductivity at any stage. The production of gases from microbial metabolisms including nitrogen, hydrogen, methane, and carbon dioxide could result in increased pressure within the DGR environment, possibly inducing fissures in the bentonite barriers [42, 46]. Conversely, other prokaryotic metabolisms, such as those associated with denitrifiers, iron-reducers, and methanogens, could be beneficial for DGR systems due to competition with SRB for electron donors, potentially decreasing SRB abundance [27, 40, 47]. Due to the possibility of MIC, as well as potential interference with other DGR barriers, it is important to investigate the activity of prevalent microorganisms in bentonite clay exposed to a variety of conditions, including both

the presence and absence of oxygen, and to determine which factors and thresholds suppress microbial growth.

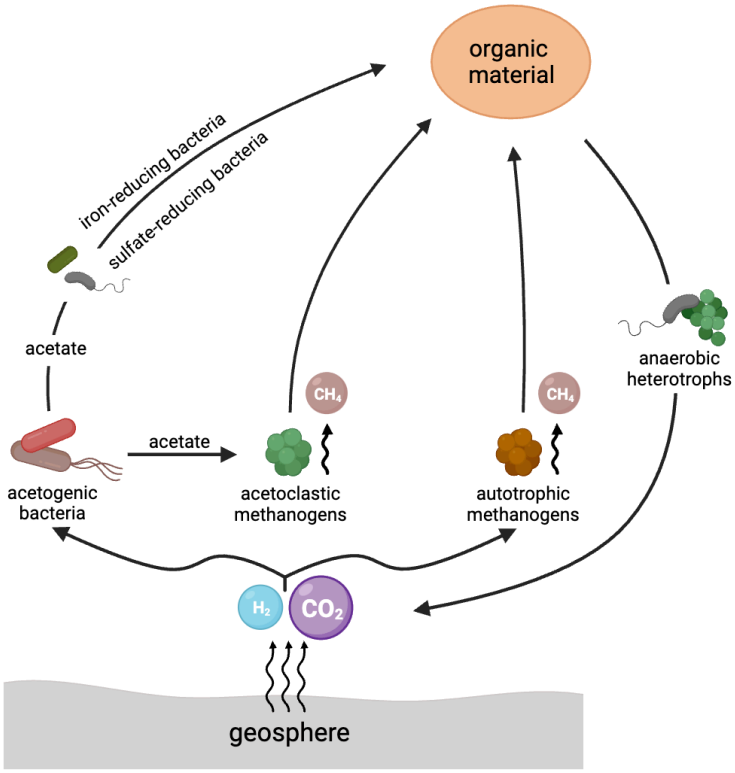


Figure 1.4. Geospheric microbiologically gas-driven cycle hypothesis, modified from elsewhere [28, 41]. Created in BioRender.com

1.6 Microbiological growth suppression in a DGR

Due to the potential of SRB-influenced MIC occurring in the repository, previous research has focused on studying the conditions in bentonite that suppress microbial growth. An important factor is water activity (a_w). Water activity is defined as the quotient of the vapour pressure of a solution ($P_{solution}$) over the vapour pressure of pure water (P_{water}; Equation 1.6), where a_w for pure water is 1.0 [29, 48]. Therefore, water activity increases as solute presence in a substance decreases. This ratio governs the availability of water for cells to use, which is an important factor influencing cell growth for both eukaryotic and prokaryotic cells [48]. It has been reported that microorganisms can grow over a range of water activities (i.e., 0.75-0.99) [20], but most bacterial cells grow readily in water activities

at 0.98 or above [20, 29, 30, 49]. Other microorganisms, such as fungi, may grow at an a_w of 0.80 [48], and halophilic bacteria are known to grow at a_w values as low as 0.75 [20, 30, 50]. Water activity is directly affected by the moisture content (MC) of a material, which is determined as the percentage of water present in a substance based on the difference between the wet mass (m_{wet}) and dry mass (m_{dry}) of that substance (Equation 1.7) [51].

Equation 1.6: $a_w = \frac{P_{solution}}{P_{water}}$

Equation 1.7: $MC = \frac{m_{wet} - m_{dry}}{m_{wet}} \times 100$

Several factors in a DGR environment can affect water activity and moisture content, including dry density, swelling pressure, and the salinity of host groundwater/infiltrating porewaters. Dry density determines adsorption of water molecules to clay particles, thus affecting the availability of free water for microorganisms [49]. As dry density increases, swelling pressure increases, determined by the load applied to the material during saturation within a fixed volume [52]. Previous studies have determined that a_w <0.96 [20, 53] and a swelling pressure >2 MPa [54] in bentonite clay suppresses microbial activity. A more recent study has used these values to demonstrate that at low salinities (<100 g/L), the *in situ* dry density of MX-80 bentonite should be ≥1.6 g/cm^3, to achieve a_w <0.96 and a swelling pressure >2 MPa. At higher salinities (>100 g/L), the a_w will be <0.96, regardless of dry density [13]. Bentonite swelling capacities decrease as concentrations of saline groundwaters increase [10, 55, 56], due to the sorption of cations onto clay particles interfering with the amount of water that will collect into interparticle spaces [10].

A short-term bentonite saturation experiment (40-90 days) [13] was also continued for an extended incubation time (~8 years) [39]. Both studies assessed microbial suppression using compacted MX-80 bentonite plugs saturated with a range of sodium chloride (NaCl) concentrations to achieve target dry densities. They determined that the abundance of culturable aerobic heterotrophs was suppressed below background levels of as-received dry bentonite (2.1 x 10^2 colony forming units; CFU/g) at a_w <0.96. In low NaCl concentrations (0

g/L and 50 g/L), culturable aerobic heterotroph abundance increased exponentially when a_w >0.96, and in high NaCl concentrations (≥100 g/L), culturability was suppressed and a_w was always <0.96 (Figure 1.5) [13, 39]. However, heterotrophic growth was detected for all experimental conditions, and this suggests a persistent presence of dormant cells or spores within bentonite clay that may grow when cultivated on laboratory culture media at relatively high water activity [13].

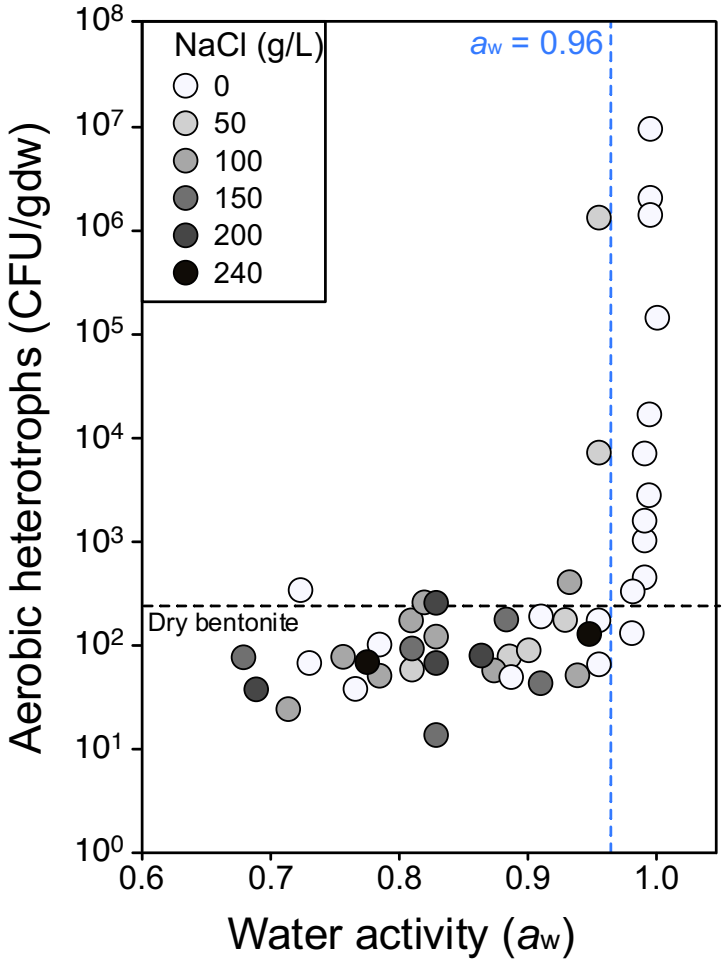


Figure 1.5. Cultured aerobic heterotroph abundance (CFU/gram dry weight) as a function of water activity in Wyoming MX-80 bentonite saturated with different salinities. Clay samples were incubated at ambient temperatures for 40-90 days before CFU analysis. Adapted from a previous publication [13].

Despite high pressures and temperatures that will be experienced in the DGR environment, specific thermophilic bacteria (e.g., sulfate-reducing *Thermodesulfobacterium*) may withstand these temperatures, and certain barotolerant species will be able to survive DGR pressure [30]. However, all microbial activity is sensitive to water availability [30], making this factor an important consideration for DGR design. Previous research spiked MX-80 bentonite with *Desulfomicrobium baculatum* and *Desulfovibrio* sp. and compacted the clay to densities corresponding to water activities of 1.0, 0.99, and 0.96, and culturable cells of both strains significantly decreased after incubation at $a_w = 0.96$ based on enumeration by the MPN method [29, 30]. Additionally, studies investigating the correlation between clay density and sulfide production found reduced sulfide production at higher densities (lower water activities) in Boom clay [57] as well as MX-80 bentonite [19, 58]. Therefore, there is a direct correlation between a_w and microbial proliferation in MX-80 bentonite, and these previously suggested parameters should be considered to prevent high rates of MIC in the DGR environment.

1.7 Geochemistry and hydrogeology of the DGR

As of August 2023, there remain two potential host sites for a Canadian DGR and both are in Ontario, Canada. The location of the host site will affect DGR specifications due to rock bed and groundwater makeup. The two potential host sites have been selected based on physical and social considerations. One host site (Ignace Wabigoon Lake Ojibway Nation) is positioned in the physiographic region of the Canadian Shield consisting of crystalline rock, whereas the other site (Saugeen Ojibway Nation-South Bruce) lies on sedimentary rock in the St. Lawrence Lowlands [59, 60]. The groundwater of either site will be influenced by the host rock composition as well as the source of the groundwater itself [60]. Depending on these factors, the groundwaters will differ in total dissolved solids (TDS) content as well as salinity.

The crystalline rock of the Canadian Shield is granitic in nature, holding a Na-Ca-SO_4-Cl type groundwater [60, 61]. During cooling of the parent magma, the primary fluids of this groundwater were most likely lost and replaced by secondary hydrothermal fluids over

time, eventually being diluted by ancient surface water infiltration. Likely, the leaching of ions over billions of years in the Canadian Shield through groundwater-granite interactions gave rise to a higher TDS content than initial infiltration waters [60]. The sedimentary rock host in the St. Lawrence Lowlands site consists of a dolostone, shale, and limestone lithology [61], also containing a Na-Ca-SO_4-Cl type groundwater [60]. This groundwater may be a result of ancient evaporated seawater that precipitated the limestone, with the potential for other infiltrating surface waters to alter the geochemistry of the groundwater [60]. Groundwaters from both crystalline and sedimentary bedrock sites are circumneutral and are associated with reducing conditions [60]. Generally, deeper groundwaters have a higher residency time and correspondingly higher TDS contents. Based on sampling data collected at or near the expected repository depth of 500 metres from each potential site, the NWMO has developed reference groundwater "recipes" to mimic the two prospective repository groundwater compositions (Table 1.1). The crystalline site reference groundwater, CR-10, has a TDS content of ~11.3 g/L [60, 62], with the sedimentary site reference groundwater, SR-270, having a TDS content of ~276.2 g/L [60, 63]. The initial SR-270 reference has since been updated to SR-290 but is not yet published, which includes changes in chemical composition, for example by adjusting the iron concentration from 30 mg/L in SR-270 to 5 mg/L in SR-290 [60, 63, 64].

Table 1.1. Major ionic composition of reference groundwaters for potential DGR host sites [60].

				Solutes (mg/L)								
Reference	pH	Eh (mV)	Ionic strength (mol/kgw)	Na	K	Ca	Mg	Fe	Cl	SO_4	HCO_3	TDS
CR-10	7.0	-200	5.78	1,900	15	2,130	60	1	6,100	1,000	70	11,300
SR-270	6.3	-200	5.88	50,025	12,486	32,494	8,173	30	168,058	1,784	135	276,184

A higher TDS content in groundwater indicates the presence of more ions and thus a more saline fluid, resulting in lower water activity due to the interaction of ions with water molecules [60]. Although these conditions are correlated with microbial suppression [13, 30, 39], certain halotolerant, spore-forming, or desiccation-resistant bacteria can survive at low

water activities and high salinities. A previously mentioned study demonstrated the survival of *Desulfovibrio africanus,* a SRB indigenous to MX-80 bentonite, at high salinities (4% NaCl) [35, 65]. Additionally, *Pseudomonas stutzeri*, a non-spore-forming and denitrifying heterotroph previously isolated from MX-80 bentonite has been found to grow in solutions containing NaCl concentrations up to 7.5% [20].

1.8 Current state of the field

1.8.1 Methods for microbiological analysis in bentonite

Early studies investigating the microbiology of bentonite clay focused on cultivation-based methods [20, 29, 30]. However, many microorganisms do not grow readily in laboratory culture, yet remain viable in their natural environments. Laboratory conditions may be more restrictive in growth time or nutrient availability than natural settings, and it is common for up to 99% of environmental microorganisms to fail to be cultivated for this reason [20, 24, 66]. For example, cells surrounded by bentonite may become desiccated, forcing microorganisms into a dormant state of non-cultivability [13, 35, 39, 65, 67, 68]. Non-cultivation-based methods that can analyze microbial abundance, such as quantitative PCR (qPCR), can provide data based on microbial gene presence and do not rely on laboratory cultures. However, such techniques can often provide an overestimation of viable microorganisms due to the presence of "relic DNA" or single genomes containing multiple copies of the 16S rRNA gene, and for this reason, gene quantification pairs well with traditional cultivation methods [24, 66, 69, 70]. Additionally, the extraction of DNA from bentonite has previously been challenging due to the low biomass present, adsorption of positively charged DNA molecules to negatively charged montmorillonite clay matrices, and the swelling nature of the clay upon contact with extraction buffers [45, 71, 72]. Studies have focused on validating the extraction of DNA from these clay matrices [45, 71], offering confidence in the use of non-cultivation-based approaches for abundance data, such as qPCR, and DNA sequencing approaches for community composition analyses. Furthermore, studies have used phospholipid fatty acid (PLFA) analyses as another method of gathering abundance data for viable cells [13, 24, 68, 73–75], as PLFAs are integral components of intact cell membranes and have been reported to degrade within minutes to hours of cell death and lysis [74, 76]. When used together, cultivation, qPCR, and PLFA data can provide

measures of microbial abundance in bentonite, with 16S rRNA gene sequencing allowing insight into the taxonomic profiles of samples.

1.8.2 Recent research

Research investigating microbial viability, abundance, and community composition in DGR-relevant conditions is widespread. For example, the Material Corrosions Test (MaCoTe) conducted at the Grimsel Underground Research Laboratory in Switzerland uses copper coupons embedded in highly compacted MX-80 bentonite cores emplaced in boreholes to assess microbial communities and corrosion potential over time [73]. Using 16S rRNA gene sequencing and PLFA analyses, microbial community stability is suggested across bentonite cores, with groups differing based on location within the core (outer versus inner core), and *Pseudomonas stutzeri* and *Streptomyces* amplicon sequence variants (ASVs) dominating microbial profiles [73]. Other experiments placing compacted bentonite in anoxic boreholes within Opalinus clay at the Mont Terri underground rock laboratory in Switzerland found persistent aerobic heterotroph abundances and low contributions from SRB [77]. Culture and sequence-based analyses of natural analogue samples from the Tsukinuno bentonite deposit in Japan, Opalinus clay in Switzerland, and crystalline rock cores from the Canadian Shield have also revealed low abundances of SRB in bentonite and the presence of heterotrophs across all samples [66]. Communities of dry, as-received bentonite samples have also been compared, including MX-80 and Asha bentonites, where cultivation and sequencing techniques determined core taxa found across samples, including heterotrophs such as *Bacillus*, and SRB such as *Desulfosporosinus* [24]. Studies also assess how conditions in bentonite, such as dry density, affect bacterial and archaeal abundance and gene profiles and seek to target other groups, such as fungi, in deep subsurface environments [18, 60, 73].

Microcosm experiments have also been used to determine the effects of various DGR conditions, including water activity and availability, on microbial activity in bentonite. For example, sulfate reduction only occurred when SRB indigenous to MX-80 or deep groundwaters had access to both liquid water and an energy source, despite having a relative humidity of 100% in the incubation airspace of sample tubes [78]. Experiments assessing

iron-reducing bacteria using high temperatures and low water activities in compacted bentonite blocks in the presence of carbon steel revealed the ability of certain spore-formers to survive unfavourable conditions expected in a DGR [40].

Another current research focus involves testing natural organic matter (NOM) chemistry of bentonite clay because the availability and types of organic carbon impact microbial growth. Geochemical analyses indicate consistency in NOM profiles across MX-80 bentonite samples and suggest relatively low carbon content, with the majority of the carbon being inorganic [79]. However, when creating an interface between compacted bentonite and a sand layer to mimic DGR conditions, it was found that the natural organic matter in bentonite has the potential to promote microbial growth and sulfate reduction [31]. These studies provide insight into potential microbial metabolisms in bentonite and possible activity that may occur in a DGR environment.

Whereas research being done in this field can be used to provide safety specifications for use in the design and construction of a DGR, to my knowledge there has been no prior research specifically investigating the independent effect of water activity on microbial growth in bentonite clay. When studying water activity in bentonite, pressure is typically tested as a factor of suppression in conjunction with water activity [13, 20, 30, 66, 73, 77]. Therefore, it is poorly understood how water activity, and concomitantly salinity, affects microbial activity and community composition in bentonite, independent of compaction or swelling pressure. It is important to study individual factors of suppression to gain a better understanding into how microorganisms may react in a DGR environment, especially during stages of variability where low pressures and high water activities might provide favourable conditions for life. This knowledge gap can be filled with the use of abundance and community composition analyses, such as cultivation techniques, qPCR, and high-throughput sequencing.

1.9 Objectives

This research investigated temporal effects of water activity, hydration media, and salinity on microbial viability, abundance, and community composition in Wyoming MX-80

bentonite clay, independent of pressure, for both oxic and anoxic conditions. The first objective was to determine how water activity affects microbial viability, growth, and community composition. This was achieved through the establishment of microcosms containing uniformly hydrated Wyoming MX-80 bentonite at low, medium, or high water activities. Cultivation, qPCR, and sequencing approaches at several timepoints allowed comparisons of microbial communities for each water activity temporally. The second objective was to investigate the effect of salinity on microorganisms in bentonite, specifically how salinity levels relevant to host site conditions affect microbial viability, growth, and community composition. This was accomplished by wetting Wyoming MX-80 bentonite clay with water, low-salinity medium ("CR-10" recipe), high-salinity medium (290 g/L NaCl), or SRB medium to target water activities. Cultivation, qPCR, and sequencing approaches were used to compare how salinity levels affected microbial viability, growth, and community composition over time. All microcosms were produced, maintained, and analyzed in either oxic or anoxic conditions to reflect a range of possible DGR conditions.

Chapter 2

Materials and methods

2.1 Bentonite hydration and microcosm set-up

As-received Wyoming MX-80 bentonite (sample bucket "MX9"; American Colloid Company) was used for microcosm establishment. Set volumes of sterile ultrapure Milli-Q water, prepared CR-10 medium (Table 1.1; NWMO), SRB medium (M803, HiMedia Laboratories, PA, USA), or prepared high-salinity medium (286.8 g/L NaCl) corresponding to target water activities (0.93, 0.96, 0.99) were pipetted onto 65 g of as-received bentonite (Table 2.1). Target water activities were based on hydration with water. Corresponding volumes of other media resulted in lower water activities depending on the TDS composition in the solution. A finalized SR-290 recipe was not yet complete when this experiment was conducted. Therefore, an equivalent TDS solution of NaCl was used due to the dominant presence of Na and Cl ions in SR-290.

Table 2.1. Volumes of water necessary to achieve specific water activities in a fixed mass of bentonite.

Bentonite (g)	Water (mL)	Water activity (a_w)
65.0	8.8	Low (~0.93)
65.0	11.4	Medium (~0.96)
65.0	19.5	High (~0.99)

Bentonite and media were hand-mixed aseptically with ethanol-sterilized gloves on an autoclaved foil surface to achieve a uniform texture. Samples were then transferred to sterile 125-mL Mason jars (Bernardin) and sealed for incubation at 30°C. Oxic microcosms were prepared on the bench and anoxic microcosms were prepared in a vinyl anaerobic chamber (COY Laboratory Products, MI, USA) filled with a 5% hydrogen 95% nitrogen gas mix, and the media used for hydration were first flushed with 100% nitrogen for ≥30 minutes/L. The hydrogen concentration was always ≥2% and the oxygen concentration was

<20 ppm during use in the chamber. Anoxic microcosms prepared in the anaerobic chamber were placed into heat-sealed polyethylene bags (127 µm; Uline) within the chamber along with GasPak EZ Anaerobe Container System Sachets (BD BBL) and GasPak Anaerobic Indicator Strips (BD BBL) to ensure anoxic conditions, and were then shuttled out for incubation at 30°C. All microcosms were opened and mixed, where ~6 g of bentonite was removed and analyzed at zero-day, three-day, one-week, one-month, three-month, and six-month timepoints, followed by resealing and incubation at 30°C. Anoxic microcosms were only opened within the anaerobic chamber and were always contained in a heat-sealed bag outside of the chamber. As-received dry bentonite microcosms were produced, maintained, and processed in the same conditions as hydrated microcosms. All microcosms were produced in duplicate.

2.1.1 Large-scale microcosms

Bentonite masses and corresponding water volumes for hydration at low (0.93) and high (0.99) water activities were scaled up ten-fold to produce large-scale microcosms. All microcosms were produced in oxic conditions and hydrated with sterile ultrapure Milli-Q water. Microcosm preparation followed the procedure from section 2.1. Bentonite samples hydrated to a low water activity were stored in water-tight, sterile 1 L Mason jars (Bernardin) and samples hydrated to a high water activity were stored in water-tight, sterile 1.9 L Mason jars (Bernardin) to account for the degree of swelling and headspace ratios. All microcosms were produced in duplicate.

2.2 Water activity and moisture content

At each timepoint, the water activity and moisture content of bentonite within each microcosm was measured. Approximately 2 g of clay was placed into a cylindrical metal or plastic cup that was <50% filled yet ensured a fully covered cup base area. A WP4C Dewpoint PotentiaMeter (Decagon Devices, WA, USA) was used on “fast mode” to measure the water activity of all samples, except for six-month timepoint samples of single replicates of anoxic microcosms hydrated with water and SRB medium, six-month timepoint samples of anoxic microcosms hydrated with CR-10, and six-month timepoint samples of oxic and anoxic microcosms hydrated with high-salinity medium, which had water activity

measurements completed with an Aqualab 4TE Water Activity Meter (METER Group, WA, USA). The WP4C Dewpoint PotentiaMeter provides a water potential output (MPa) as well as temperature (°C), and these values were converted (Pa, K) and used to calculate water activity according to manufacturer instructions using Equation 2.1.

Equation 2.1: $a_w = e^{[(\text{Pa x } 0.000018)/(\text{K x } 8.3143)]}$

After water activities were measured, bentonite samples within the plastic or metal cups were weighed and baked in foil cups in an oven at 110-115°C for ≥24 hours to calculate the moisture contents by dividing the weight of water lost by the original (dry) weight of the bentonite (x100) using Equation 2.2.

Equation 2.2: $\text{MC} = \frac{m_{wet} - m_{dry}}{m_{wet}} \text{ x } 100$

2.3 Cultivation

At each timepoint, aerobic heterotroph, anaerobic heterotroph, and SRB counts were conducted. Using 2 g of clay added to 18 mL phosphate-buffered saline (PBS), a 1:10 dilution slurry was made and vortexed at a low speed for 30 minutes. A ten-fold dilution series was prepared from this slurry (up to 1:1 000, 1:10 000, or 1:100 000 depending on the microcosm). Cultures from oxic microcosms were cultivated on the bench in oxic conditions, and anoxic microcosm cultures were cultivated in the anaerobic chamber. The hydrogen concentration was always ≥2% and the oxygen concentration was <20 ppm during use in the chamber. Significant differences between cultivation data were identified based on 95% confidence intervals, where overlapping intervals indicated no significant difference between data.

2.3.1 Heterotrophs

Triplicate agar plates were prepared from each dilution (up to 1:100, 1:1000, 1:10 000, or 1:100 000 depending on the microcosm) for aerobic heterotrophs and from dilutions 1:10 or 1:100 for anaerobic heterotrophs. From selected dilutions, 100 µL was pipetted onto Reasoner's 2 Agar (R2A; M1687, HiMedia Laboratories, PA, USA) plates and spread using

a sterilized glass spreader or sterile glass beads (4 mm) until the agar surface was dry. Aerobic heterotroph plates were incubated in oxic conditions at 30°C for 5-7 days. Anaerobic heterotroph plates were shuttled into heat-seal polyethylene bags (127 µm; Uline) along with GasPak EZ Anaerobe Container System Sachets (BD BBL) and GasPak Anaerobic Indicator Strips (BD BBL) to ensure anoxic conditions. For anoxic cultivation, bags were flushed with a 10% carbon dioxide 90% nitrogen gas mixture followed by heat sealing. All bags were then stored at 30°C for 28 days. After designated incubation times, plates were enumerated by colony counting, and CFU per gram dry weight (gdw) was calculated using the moisture content of the bentonite sample from where the cultures originated. A representative swab of all colony morphologies present on the plates was taken and frozen alone or in 200 µL PCR water at -20°C for downstream DNA analyses.

2.3.2 Sulfate-reducing bacteria

Five tubes containing 9 mL SRB medium (M803, HiMedia Laboratories, PA, USA) were inoculated with 1 mL from each dilution (up to 1:1000, 1:10 000, or 10:100 000). Tubes were shuttled into steel anaerobic vacuum chambers (Best Value Vacs) along with GasPak EZ Anaerobe Container System Sachets (BD BBL) and GasPak Anaerobic Indicator Strips (BD BBL) to ensure anoxic conditions. Chambers were purged and flushed with a 10% carbon dioxide 90% nitrogen gas mixture and were incubated at 30°C for 28 days. Sulfate-reducing bacteria were estimated via the most probable number (MPN) method using a five-tube MPN table [80] based on the presence of a black precipitate (iron sulfide). The most probable number of SRB per gram dry weight was calculated using the moisture content of the bentonite sample from which the cultures originated. From each positive tube, 1 mL was aliquoted, pelleted, and the pellet frozen at -20°C for downstream DNA analyses.

2.4 DNA extraction and quantification

2.4.1 Microcosm bentonite samples

All extractions of DNA from bentonite were completed in an ISO 5 HEPA filtered PCR hood (AirClean Systems, ON, CA) that was cleaned with 80% ethanol and treated with UV light for 15 minutes. At each timepoint, genomic DNA was extracted from 50 ± 0.9 mg of microcosm bentonite samples using DNeasy PowerSoil Pro kits (Qiagen) according to

manufacturer instructions, and the protocol used for extractions from MX-80 bentonite was previously validated [71]. After the addition of lysis buffer, extraction tubes were incubated at 70°C in a rotating incubator for 10 minutes, followed by a bead-beating step at 5.5 m/s for 45 seconds using a FastPrep instrument (MP Biomedicals). The extracted DNA was eluted in 50 µL of elution buffer. Quantification of extracted DNA was carried out using a Qubit 4.0 fluorometer (Life Technologies, CA, USA), but the DNA content was often below the detection limit of the machine. Each extract was separated into two 25 µL aliquots that were stored at –20°C until further downstream analysis. For each batch of extractions, a positive control consisting of soil or *Saccharomyces cerevisiae* yeast and a negative kit control was included.

2.4.2 Cultures

Using 50 µL of PCR water vortexed with swabs from R2A plate colonies as well as 20-50 µL of pellets from positive SRB tubes, genomic DNA was extracted from biomass cultured from oxic microcosms hydrated with water or SRB medium up to the three-month timepoint. UltraClean Microbial kits (Qiagen) were used according to manufacturer instructions. After the addition of lysis buffer, extraction tubes were incubated at 70°C in a rotating incubator for 10 minutes, followed by a bead-beating step at 5.5 m/s for 45 seconds using a FastPrep-24 instrument (MP Biomedicals). The extracted DNA was eluted in 60 µL of elution buffer and each extract was stored at –20°C until further downstream analysis. A negative kit control was included for each batch of extractions.

2.5 Quantitative PCR

All qPCR amplifications were completed in an ISO 5 HEPA filtered PCR hood (AirClean Systems, ON, CA) that was cleaned with 80% ethanol and treated with UV light for 15 minutes. The V3-V5 region of the 16S rRNA gene of *Thermus thermophilus* was previously cloned into the pUC57-Kan vector using primers M13F/M13R, followed by amplification, purification, and quantification on a Qubit 4.0 fluorometer (Life Technologies, CA, USA). A standard curve was generated from this gene fragment in a dilution series for use in qPCR quantification of samples.

Universal 16S rRNA gene primers 341F and 518R [81] were used for qPCR amplification. Each qPCR contained 15 µL total volume including 2 x SsoAdvanced Universal SYBR Green Supermix (Bio-Rad), 100 µM of each primer, 10 mM Bovine serum albumin (BSA), PCR water, and 2 µL template DNA. Each sample was quantified in duplicate. The qPCR was completed using a CFX Opus 96 Real-Time PCR System (Bio-Rad) at 98°C for 3 minutes, followed by 40 cycles of 98°C for 15 seconds, and 55°C for 30 seconds. No template controls (NTCs) included a qPCR mixture with no template DNA, and a mixture with 2 µL PCR water. Gene copy numbers were calculated using cycle threshold values determined by the standard curve, and copies per gram dry weight were calculated using the moisture content of the bentonite from where the sample originated. Significant differences between 16S rRNA gene quantification data were identified based on 95% confidence intervals, where overlapping intervals indicated no significant difference between data.

2.6 Amplification and high-throughput sequencing of the 16S rRNA gene

The PCR amplification of each sample was carried out in an ISO 5 HEPA filtered PCR hood (AirClean Systems, ON, CA) that was cleaned with 80% ethanol and treated with UV light for 15 minutes. The V4-V5 region of the 16S rRNA gene was amplified using primers 515F-Y [82] and 926R [83], modified to contain a unique 6 base index sequence that was used for flow cell binding and sequencing sites [84]. Each sample was amplified in triplicate. Amplification was conducted using a 25 µL PCR mixture containing 1 x ThermoPol Buffer, 0.2 µM primers, 200 µM dNTPs, 15 µg BSA, 0.625 units of hot start *Taq* polymerase (New England Biolabs, MA, USA), and 1 µL template DNA (undetectable to 1 ng for clay, undetectable to 20 ng for cultures, based on Qubit measurements). The PCR amplification was completed using a T100 Thermal Cycler (Bio-Rad), denaturing at 95°C for 3 minutes, followed by 40 (clay) or 35 (cultures) cycles of 95°C denaturation for 30 seconds, 55°C annealing for 3 minutes, and extension at 68°C for 1 minute, and a final extension at 68°C for 7 minutes. Preparations of NTCs were included within the 96-well plate as well as in separate tubes to control for contamination with the PCR mixture. A 1:1 plasmid-DNA mixture of the 16S rRNA gene regions of *Thermus thermophilus* and *Aliivibrio fischeri* cloned separately into a pUC57-Kan plasmid was used as a positive control.

Amplification products of all samples, NTCs, and extraction negative controls were quantified using agarose gel electrophoresis, and samples were normalized and pooled to produce the sequencing library, followed by purification using Wizard SV Gel and PCR Clean-Up System (Promega, WI, USA). Based on Illumina guidelines (Document 15039740, version 01), the library was then denatured and diluted. A lack of amplification seen on the agarose gel for many samples from the second of two sequencing runs required several samples to be removed from sequencing in order to avoid library dilution. Any sample with amplification and all zero-day and six-month timepoints were included in the sequencing run regardless of amplification yield.

A 2 x 25-cycle MiSeq Reagent Kit v2 (Illumina Canada Inc, NB, CA) was used to sequence an 8 pM library containing 15% PhiX control v3 (Illumina Canada, NB, CA) on a MiSeq (Illumina, CA, USA). The first sequencing run containing DNA from bentonite and cultures had a cluster density of 524 ± 38 and a passing filter of 93.65. The second sequencing run containing DNA only from bentonite had a cluster density of 814 ± 24 with a passing filter of 96.24.

2.7 Sequence analysis

Demultiplexing of sequences was carried out using MiSeq Reporter software (version 2.6; Illumina). Sequence analysis was processed using Quantitative Insights Into Microbial Ecology (QIIME2; version 2020.6) [85] managed by an interactive web interface (Automation, eXtension, and Integration Of Microbial Ecology; AXIOME3) [86]. Primer removal and truncation of low-quality reads past 250 base pairs (forward and reverse reads) as well as denoising was completed using the DADA2 pipeline [87]. Taxonomy was assigned to individual amplicon sequence variants (ASVs) using a naive Bayes classifier pre-trained with SILVA database release version 138 [88]. Sequences from each run were processed with Decontam [89], an R package used to identify putative contaminant sequences based on extraction and sequencing controls. The identified contaminant ASVs were removed from each ASV table. The ASV tables from the two separate sequencing runs were then merged for downstream analyses.

All sequences used in this study were deposited in the European Nucleotide Archive under project accession number PRJEB64179. Final merged ASV tables are also available (https://doi.org/10.6084/m9.figshare.23643540.v1).

An indicator species analysis was carried out in RStudio (RStudio version 2023.03.1+446, R version 4.3.0) [90] using package "indicspecies" [91] which assesses the statistical significance of the association of specific ASVs to environmental sites using occurrence and abundance data. A multi-level pattern analysis was used to identify indicator ASVs in individual sites as well as combinations of sites using function "multipatt()" [92].

2.8 Quantification of fungi

All qPCR amplifications were completed in an ISO 5 HEPA filtered PCR hood (AirClean Systems, ON, CA) that was cleaned with 80% ethanol and treated with UV light for 15 minutes. A 1000 base pair fragment of the fungal 18S rRNA gene of *Saccharomyces cerevisiae* was previously created using primers EMP515F [93] and UNI1392R, followed by amplification and quantification on a Qubit 4.0 fluorometer (Life Technologies, CA, USA). A standard curve was generated from this gene fragment in a dilution series for use in qPCR quantification of samples.

Fungal 18S rRNA genes were used for qPCR amplification using forward and reverse FungiQuant primers [94]. Each qPCR contained 15 µL total volume including 2 x SsoAdvanced Universal SYBR Green Supermix (Bio-Rad), 100 µM of each primer, 10 mM Bovine serum albumin (BSA), PCR water, and 2 µL template DNA. Each sample was quantified in duplicate. The qPCR was completed using a CFX Opus 96 Real-Time PCR System (Bio-Rad) at 95°C for 3 minutes, followed by 40 cycles of 94°C for 30 seconds, 62°C for 30 seconds, and 72°C for 45 seconds. No template controls (NTCs) included a qPCR mixture with no template DNA, and a mixture with 2 µL PCR water. Gene copy numbers were calculated using cycle threshold values determined by the standard curve, and copies per gram dry weight were calculated using the moisture content of the bentonite from where the sample originated.

Chapter 3

Results and discussion

3.1 Bentonite hydration

For establishment of the microcosms used in this study, as-received Wyoming MX-80 bentonite clay was incubated to assess microbial viability, abundance, and community composition over time. Upon uniform hydration of the material, samples visually exhibited a degree of swelling correlated with the volume of liquid added (Figure 3.1). Across all timepoints and oxygen conditions, bentonite hydrated to each target water activity with water, CR-10, or SRB medium had consistent water activity and moisture content values (Figure 3.2). Bentonite was hydrated with high-salinity medium containing NaCl that reflected the TDS content of SR-290 solution, as Na and Cl ions are dominant constituents in the SR-290 composition. Bentonite hydrated with this high-salinity solution possessed a lower water activity due to the high TDS content of the medium. Starting material MX-80 had the lowest water activity and moisture content values across all timepoints and oxygen conditions.

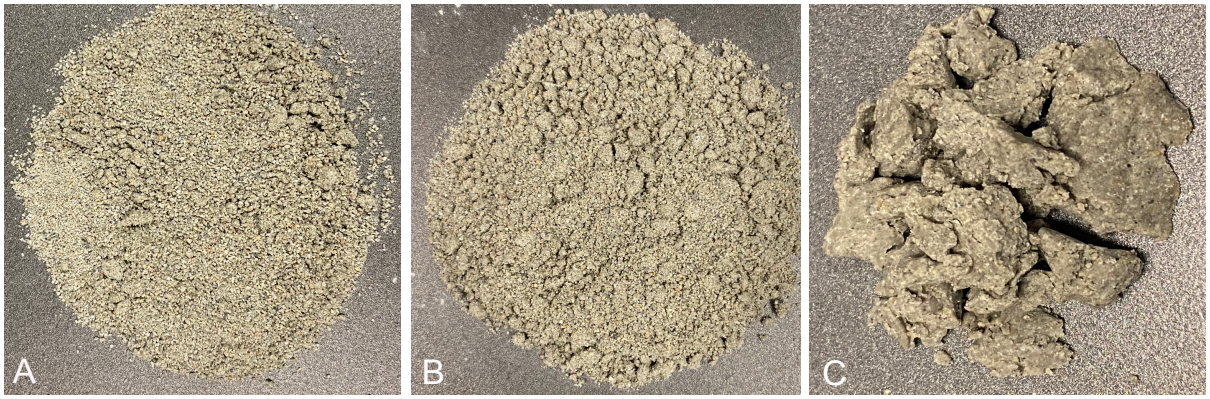


Figure 3.1. Uniformly hydrated bentonite samples at A) low (0.93), B) medium (0.96), and C) high water activities.

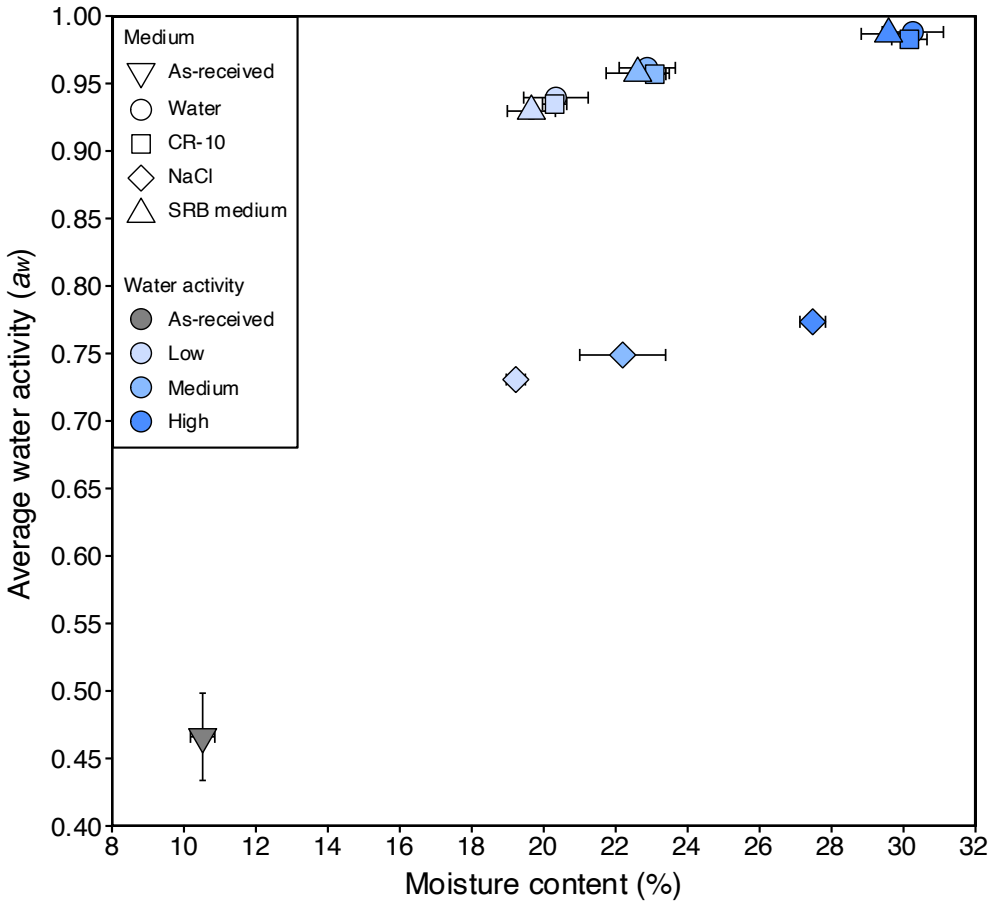


Figure 3.2. Average water activity and moisture content measurements of bentonite samples from each medium and target water activity. Each point is based on 24 samples, including all timepoints, oxygen conditions, and duplicate microcosms. Error bars represent the standard deviation between all readings for each condition across all timepoints.

Across all samples and timepoints, including both oxygen conditions, water activity readings were comparatively stable (Figure 3.3). For all timepoints and oxygen conditions, the bentonite hydrated to target water activities with water, CR-10, or SRB medium had similar and consistent water activity readings, ranging from 0.913 to 0.951 for low water activities, 0.951 to 0.966 for medium water activities, and from 0.970 to 0.992 for high water activities. The bentonite hydrated with high-salinity media experienced lower water activity readings ranging from 0.721 to 0.745 for low water activities, 0.735 to 0.759 for medium water activities, and from 0.762 to 0.786 for high water activities. The average standard deviation in each water activity for each medium across all timepoints and oxygen conditions was 0.006 for a_w, and 0.625 for moisture contents. There was a higher level of variation in water activity for samples from starting-material MX-80, ranging from a water activity of 0.432 to 0.526. This variation was most likely due to heterogeneity within the dry clay or from the dry clay absorbing moisture from the ambient air and differences in the relative humidity between oxic and anoxic conditions. Still, these results demonstrate that the process of establishing microcosms was consistent and that the microcosm jars remained gas-tight for the duration of the experiment.

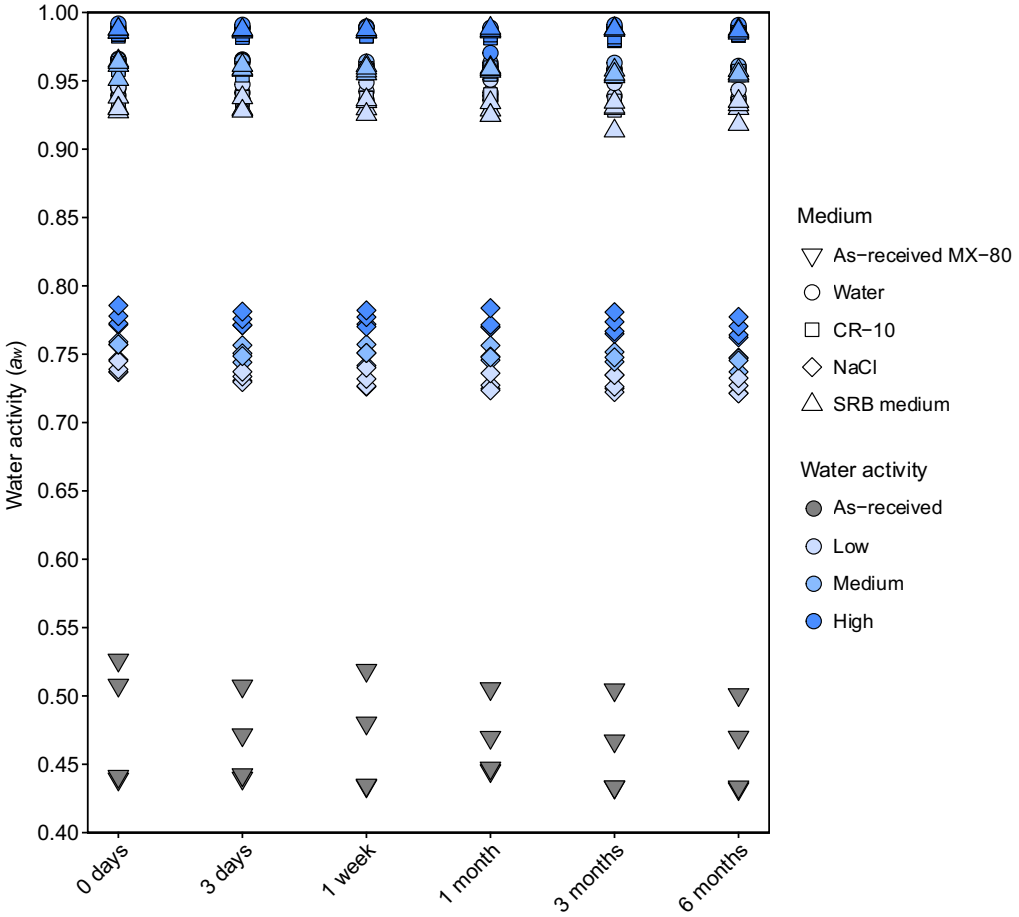


Figure 3.3. All water activity and moisture content measurements in each medium, oxygen condition, and target water activity across time.

3.2 Microbial viability and abundance

For each target water activity and all media, the abundance of 16S rRNA genes, culturable aerobic and anaerobic heterotrophs, and SRB were assessed for both oxic and anoxic incubations over six months. For oxic microcosms (Figure 3.4), microcosms hydrated with SRB medium were associated with a larger increase in abundance in the 16S rRNA gene in high water activity microcosms by the three-day timepoint.

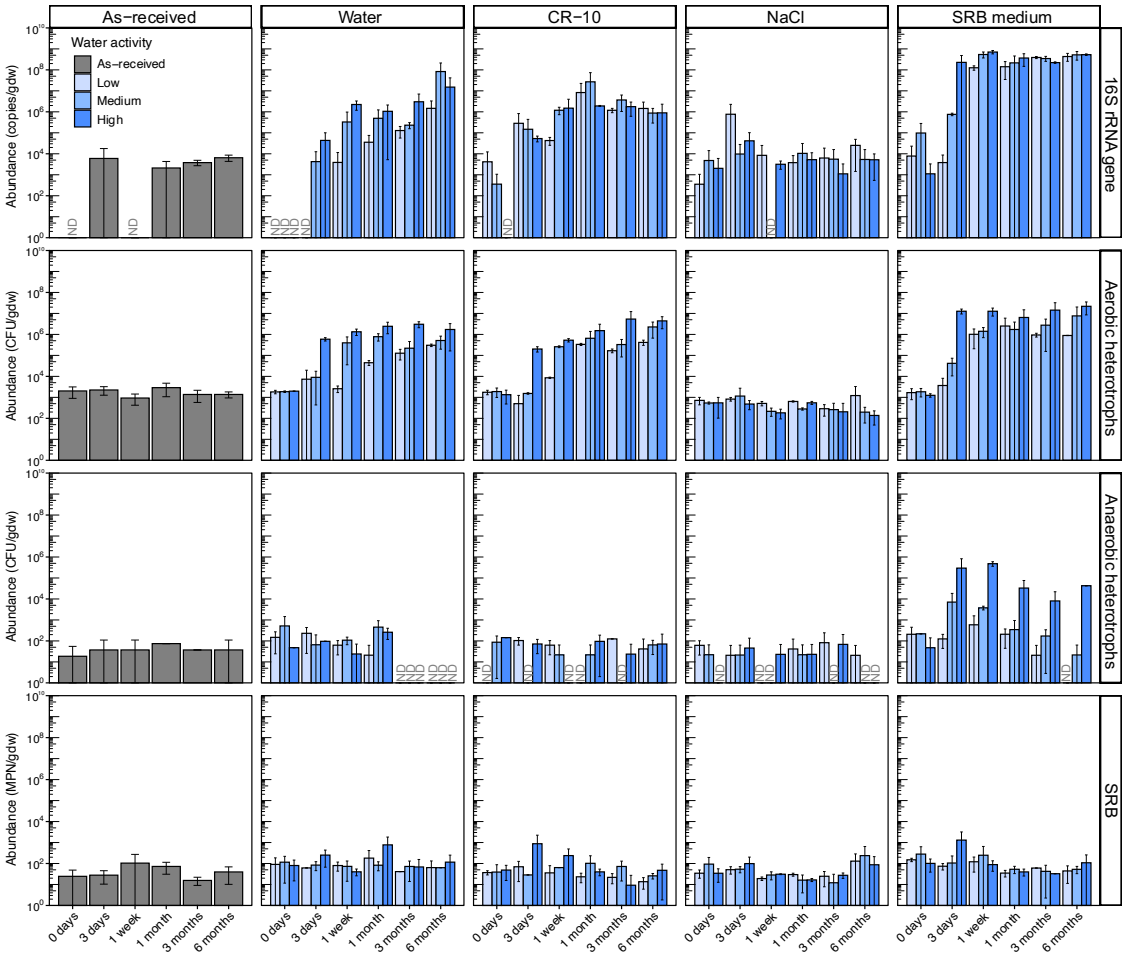


Figure 3.4. Average abundances of the 16S rRNA gene (copies/gdw), aerobic heterotrophs (CFU/gdw), anaerobic heterotrophs (CFU/gdw), and SRB (MPN/gdw) from as-received bentonite or hydrated oxic microcosms at low, medium, and high water activities. Error bars represent 95% confidence intervals between the average of biological replicates. The lower limit of quantification (background level) for heterotrophs is 2.5 x 10^3 CFU/gdw. No detectable amplification or growth is indicated by "ND".

This was reflected in culturable aerobic heterotrophs, where average abundances significantly increased (based on 95% confidence intervals) in the high water activity microcosms by day three. In contrast, microcosms hydrated to a low water activity with SRB medium were not significantly higher in abundance until the one-week timepoint for both 16S rRNA gene abundances as well as culturable aerobic heterotrophs. Average aerobic

heterotroph abundances in microcosms hydrated with water and CR-10 show a similar trend, where only the high water activity microcosms significantly increase in abundance by day three compared to day zero, and always remain greater than low water activity abundances across time. These abundances correspond with culturable aerobic heterotroph data previously seen at high water activities in bentonite samples kept at low pressure (dry density <1.00 g/cm^3) and hydrated with low salinity [13]. However, microcosms hydrated to a low or medium a_w had higher abundances in this experiment by several orders of magnitude than previously seen when pressure was included [13, 39]. This may be due to the removal of pressure as a factor of microbial suppression, allowing a greater degree of proliferation to occur despite low water activity conditions.

For all water activities, microcosms hydrated with SRB medium had greater average 16S rRNA gene abundances than other media by nearly one order of magnitude or higher by the one-week timepoint. Average 16S rRNA gene abundances did not significantly increase for any microcosm hydrated with high-salinity medium, and culturable aerobic heterotroph abundances remained constant over time as well in these samples. Culturable anaerobic heterotrophs did not increase in water, CR-10, or high-salinity medium, and counts were below the lower limit of quantification (2.5 x 10^3 CFU/gdw) or plates had no detectable growth. The average abundance of culturable anaerobic heterotrophs in high water activity microcosms hydrated with SRB medium increased from 4.7 x 10^3 to 3.0 x 10^5 CFU/gdw by the three-day timepoint. Overall, aerobic heterotroph abundances were always higher than anaerobic heterotroph abundances, which is commonly seen in bentonite cultivation data [24, 77]. For all media and water activities, average SRB abundances did not increase throughout the six-month incubation.

Abundances in as-received MX-80 bentonite clay remained constant, and average abundances at the zero-day timepoint for all media and water activities were not significantly different from starting materials. The abundance data of as-received dry clay are comparable to values previously seen for dry uncompacted bentonite [24].

Microcosms hydrated to a higher water activity had increased microbial abundances, presumably due to favourable water availability conditions allowing microbial proliferation in comparison to water activities that have been identified previously to induce microbial suppression in bentonite ($a_w < 0.96$) [13]. Microcosms hydrated with SRB medium most likely had higher average abundances in both 16S rRNA gene copies and culturable heterotrophs due to the high nutrient content provided by the medium, including lactate as an energy and carbon source [29, 30, 95]. Because there is low organic carbon content in MX-80 bentonite [5, 79], the additional nutrients provided by SRB medium would have allowed increased and faster proliferation to take place even in low water activities, specifically of aerobic heterotrophs, than in bentonite hydrated with water or saline media. This is seen in the significant increase by the one-week timepoint of the 16S rRNA gene and culturable aerobic heterotrophs in low water activities experienced in microcosms hydrated with SRB medium compared to water or CR-10. Microbial abundances may have reached a "steady state" in all microcosms over time because of exhaustion of available water or nutrient requirements. Microcosms hydrated with the high-salinity medium had a much lower a_w than most microorganisms require [20, 29, 30, 49] due to the binding of ions with available water. Baseline abundances of viable microorganisms detected in those microcosms were not different from as-received starting materials and likely reflect spore germination or growth of desiccation-resistant bacteria that persist in the material.

For anoxic microcosms, average abundances of 16S rRNA gene copies, culturable aerobic and anaerobic heterotrophs, and SRB enrichments remained constant over time in all conditions and were comparable to as-received starting material abundances (Figure 3.5). Additionally, many aerobic and anaerobic heterotroph counts were below the lower limit of quantification (2.5×10^3 CFU/gdw) or plates had no detectable growth. A lower abundance of aerobic heterotrophs was seen due to the lack of oxygen availability in the microcosms and during incubation, and microorganisms that did form colonies may have existed as spores or facultative anaerobes [49, 96]. Anoxic microcosms had lower overall microbial community abundances when compared to oxic microcosms. Abundances of the 16S rRNA gene, aerobic heterotrophs, and SRB were significantly lower in anoxic microcosms (Mann-

Whitney U test, p <0.05), whereas anaerobic heterotroph abundances were similar across oxygen conditions (Mann-Whitney U test, p >0.05).

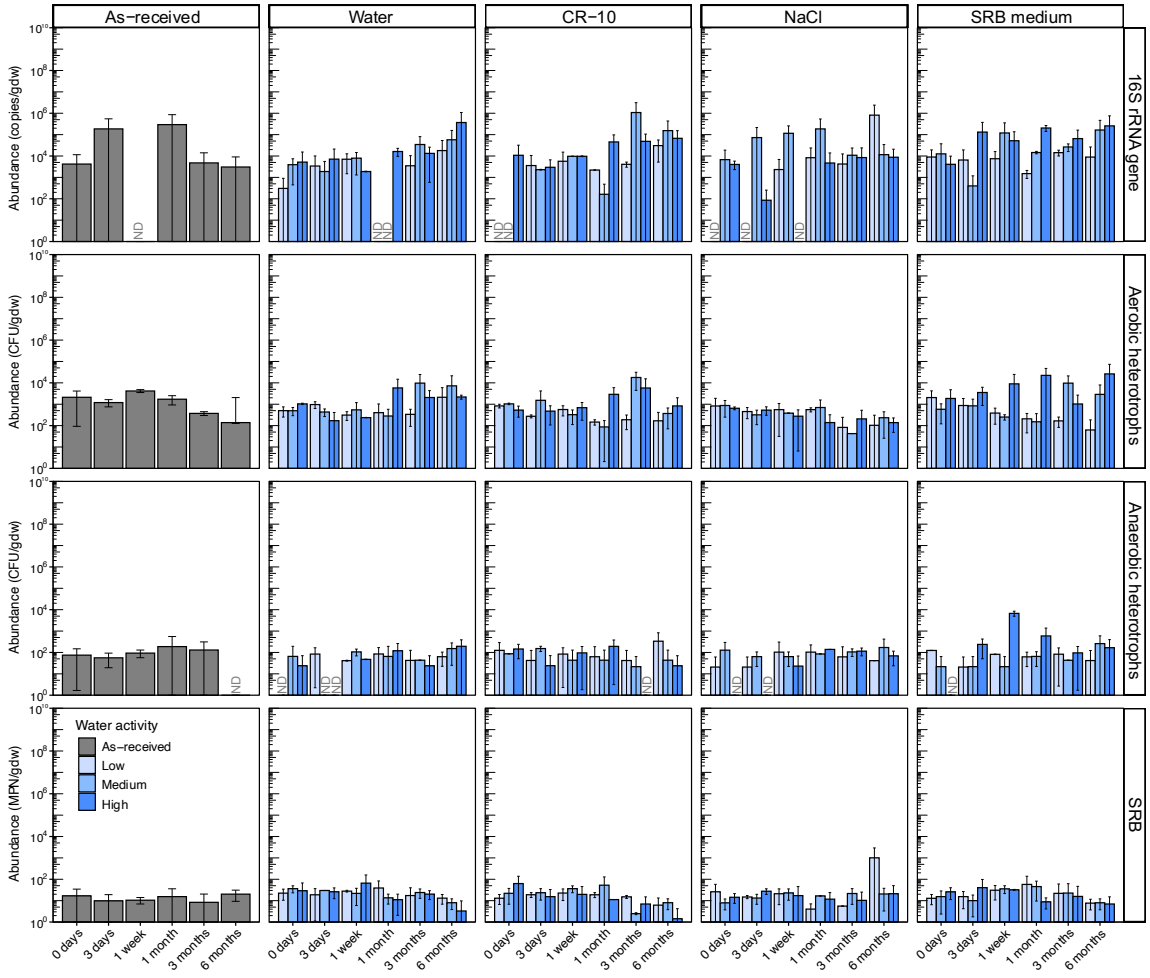


Figure 3.5. Average abundances of the 16S rRNA gene (copies/gdw), aerobic heterotrophs (CFU/gdw), anaerobic heterotrophs (CFU/gdw), and SRB (MPN/gdw) from as-received bentonite or hydrated anoxic microcosms at low, medium, and high water activities over time. Error bars represent 95% confidence intervals between the average of biological replicates. The lower limit of quantification (background level) for heterotrophs is 2.5 x 10^3 CFU/gdw. No detectable amplification or growth is indicated by "ND".

Lower abundances of aerobic heterotrophs in oxic microcosms corresponding with low water activities and increased salinity suggests that low water activity in a DGR will contribute to suppression of microbial growth that, when combined with pressure in a DGR, will further restrict microbial proliferation. Anaerobic culture abundances, as well as all anoxic microcosm data, also indicate that once anoxic conditions are established in a DGR environment, microbial proliferation will be minimal, especially in low nutrient environments. However, this does not eliminate the possibility that microbial abundances could increase during periods of variability in the DGR or at interface locations where water activity, pressure, and temperature may fluctuate and provide favourable growth conditions.

Although anaerobic SRB were expected to grow within anoxic microcosms, especially when hydrated with a high nutrient SRB medium, the abundance of SRB abundances for all conditions and timepoints were significantly higher in oxic microcosms rather than anoxic microcosms. Nevertheless, abundances of SRB in both oxic and anoxic conditions remained low overall. There may be certain inhibitory factors in bentonite preventing SRB proliferation [77]. *Desulfomicrobium baculatum*, a species of SRB, has previously been seen to survive in compacted bentonite after 60 days of non-limiting conditions (i.e., a_w =1.0). However, only ~10% of the original population remained and the authors suggested that limited nutrients and an accumulation of hydrogen sulfide constrained microbial viability [29, 30]. Nevertheless, this does not account for the lack of survival at high water activities in this project because there was no indication that high concentrations of hydrogen sulfide inhibited SRB growth in these microcosms. Hydrogenotrophic growth has been reported for autotrophic SRB, including *Desulfosarcina variabilis*, *Desulfonema limicola,* and *Desulfococcus niacini* [29], which have not been frequently reported in MX-80 bentonite. However, previous studies have shown that SRB rapidly oxidize hydrogen for sulfate reduction in Opalinus clay and Bavarian bentonite [46, 97]. The >2% hydrogen headspace provided in anoxic microcosm jars may support autotrophic SRB presence and viability; however, this concentration may not be high enough to fully diffuse the bentonite clay matrix. It is therefore likely that there was a lack of hydrogen for autotrophic SRB, or that the bentonite matrix itself inhibited SRB proliferation, specifically in anoxic conditions.

Future research should test SRB culture incubations using a hydrogen gas headspace or bentonite additions to pure culture representatives to investigate this hypothesis.

For all microcosm conditions, the average abundances of the 16S rRNA gene were always significantly higher than corresponding cultivation-based estimates of CFU or MPN (Wilcoxon signed ranks test, $p < 0.05$; Figure 3.4, Figure 3.5). This is most likely due to both the presence of relic DNA in the bentonite samples or multiple copies of the 16S rRNA gene within singular genomes, as well as the inability of certain microorganisms to be cultured in a laboratory environment, including most actinobacterial species [98–101]. These factors provide a potential over-estimation of abundance data for cultivation-independent approaches, and limiting abundance data for cultivation approaches. Previous estimates indicate that relic DNA can account for an average of up to 40% of prokaryotic and fungal DNA in soil [102, 103], but it is debated if this relic DNA significantly alters microbial community composition profiles [102, 104]. Other culture-independent methods of quantification focus on targeting the abundance of viable microorganisms alone, such as PLFA analyses. Bioluminescent adenosine triphosphate (ATP) assays use ATP as a marker for cellular viability [66, 105–107] and has been used previously in subsurface environments, including bentonite and other clays [18, 107, 108]. Additionally, DNA-binding dyes, including propidium monoazide (PMA), can distinguish extracellular DNA from intact cellular membranes and have been used to inhibit the amplification of relic DNA in qPCR [66, 109–111]. These methods should be further optimized for use in bentonite and these types of experiments.

3.3 Microbial community composition

3.3.1 16S rRNA gene sequencing run comparison

The 16S rRNA gene was sequenced from samples in two sequencing runs. Bentonite samples in the first sequencing run were sequenced alongside culture samples and consisted entirely of oxic microcosm samples hydrated with water and SRB medium up to the 3-month timepoint. These samples were generally higher in biomass, as seen in culture-based data (Figure 3.4), when compared to bentonite hydrated with high-salinity media and bentonite from all anoxic microcosms, which were sequenced in the second run. Many of these lower

biomass samples included in the second run did not have visible PCR products in an agarose gel prior to sequencing. To prevent such low amplification samples from diluting the pooled library for sequencing, only replicates of samples showing any amplification, as well as all samples from zero-day and six-month timepoints, were included in the second sequencing run (Figure 3.6). For all samples sequenced in both runs, read counts of the 16S rRNA gene ranged from 0 reads to 2.1×10^4 reads. Average read counts were lower for as-received MX-80 starting material samples, samples hydrated with high-salinity medium, samples at the zero-day timepoint, and samples from anoxic microcosms when compared to all other samples (Figure 3.7). Average reads of DNA-extraction negative kit controls and NTCs revealed an average of 1.0×10^1 reads in the first run and an average of 3.9×10^2 reads in the second sequencing run. Potential contaminant ASVs associated with DNA-extraction negative controls and PCR NTCs (28 negative controls in run one; 32 negative controls in in run two) were identified through Decontam, resulting in the removal of eight contaminant ASVs out of 1,268 from samples sequenced in run one, and 36 ASVs out of 990 from samples sequenced in run two. It is likely that sequencing run two had a higher level of contamination as contaminant DNA from exogenous sources disproportionately affects samples with lower biomass [89, 112, 113]. Overall, these raw sequencing data reinforce 16S rRNA and culture abundance data suggesting minimal microbial viability and proliferation occurring in samples hydrated with high-salinity medium and samples incubated under anoxic conditions.

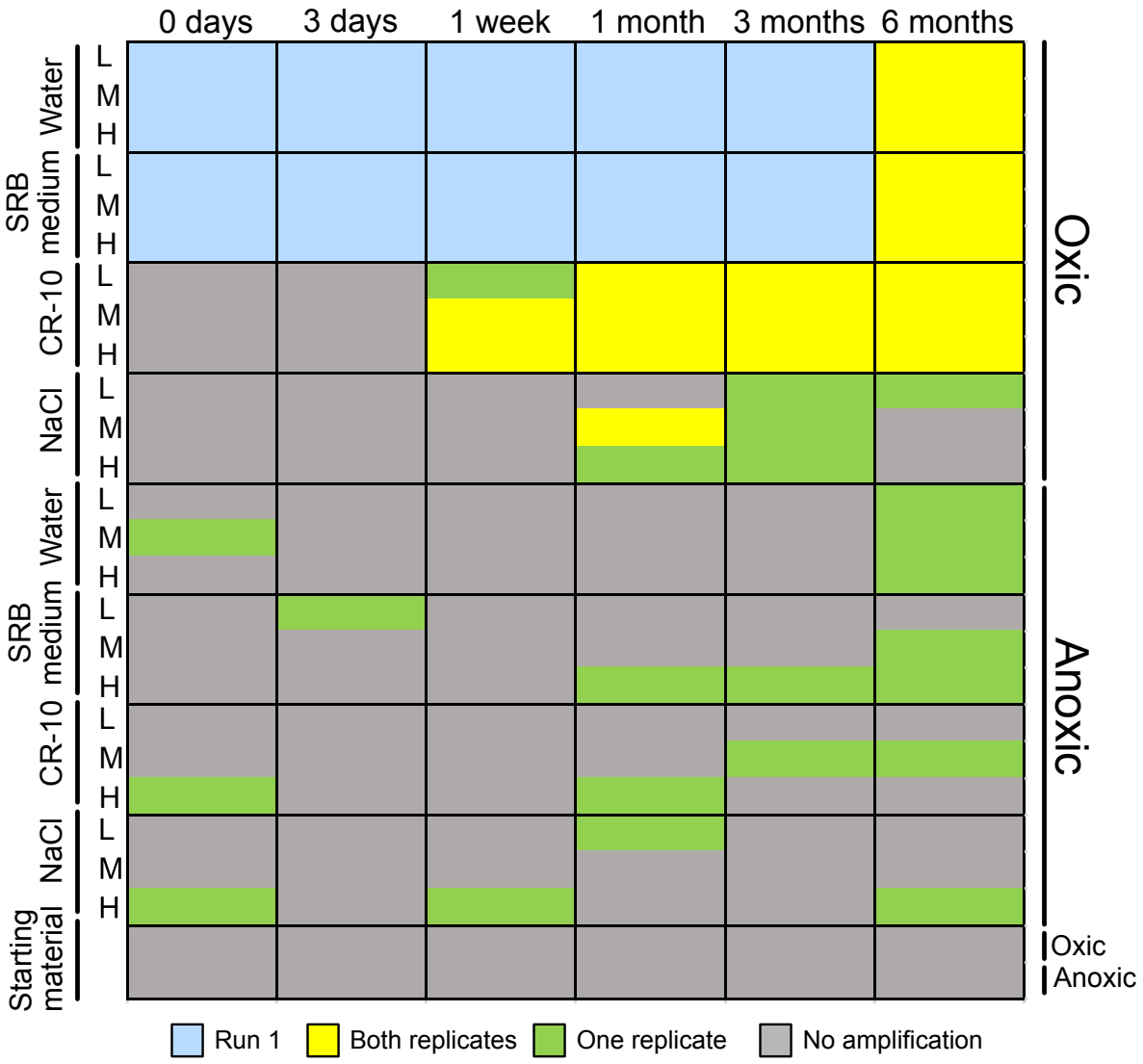


Figure 3.6. PCR amplification of samples including microcosms hydrated with each medium at low (L), medium (M), or high (H) water activities from sequencing run two based on visual agarose gel electrophoresis bands. All samples coloured in yellow and green, as well as all grey zero-day or six-month timepoint samples were included in sequencing run two.

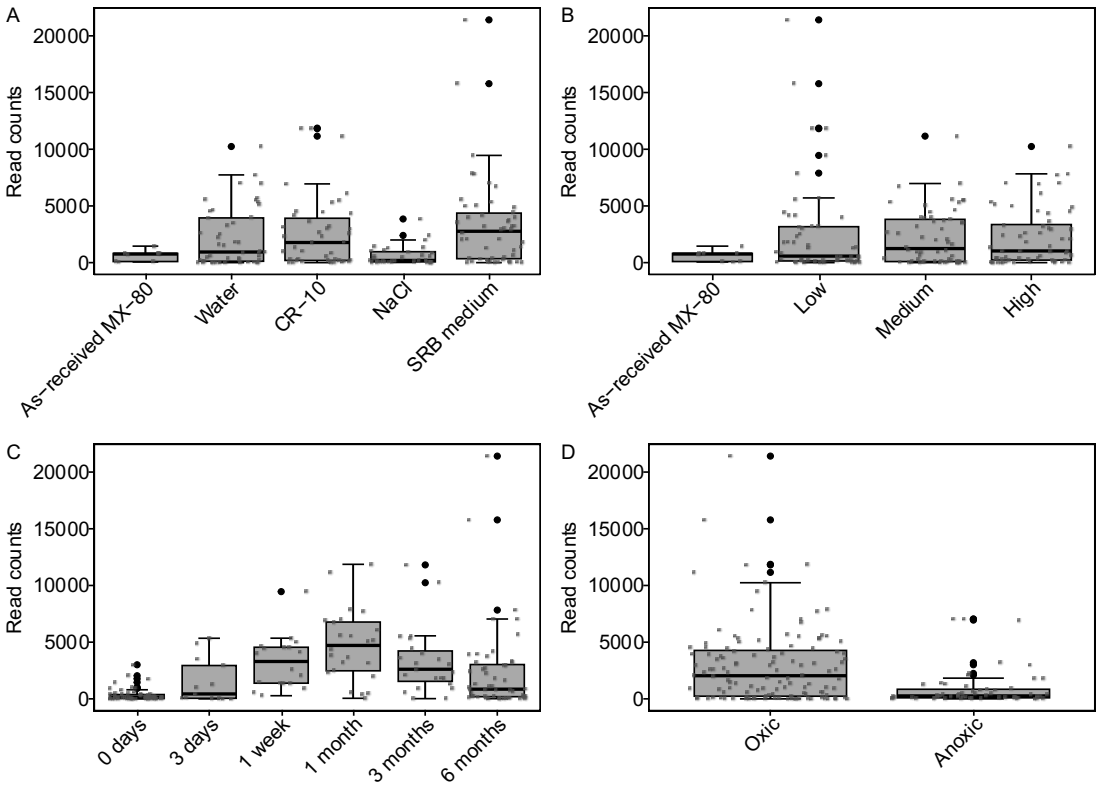


Figure 3.7. Boxplots with a jitter overlay displaying average read counts from 16S rRNA gene sequencing compared across all bentonite samples within A) each hydration medium, B) each water activity, C) each timepoint, and D) both oxygen conditions.

3.3.2 Microbial community composition of microcosm samples

Microbial community profiles based on ASVs from sequencing of the 16S rRNA gene revealed a dominance of the phylum *Actinobacteriota*, specifically in oxic microcosms hydrated with water, CR-10, and SRB medium. After rarefaction to 2040 reads, all sequenced samples grouped mostly by water activity (Figure 3.8 A) and oxygen conditions (Figure 3.8 B) and less by different media (Figure 3.8 C) or timepoints (Figure 3.8 D). Oxic microcosm sample profiles were more dissimilar across water activities than for anoxic microcosm profiles (Figure 3.8 A, B), and three oxic samples from microcosms hydrated with high-salinity medium or SRB medium at zero days grouped closely with the anoxic sample group. This is most likely due to the lack of microbial proliferation experienced in these lower biomass samples, as based on cultivation data, anoxic microcosms as well as microcosms hydrated with high-salinity medium or at early timepoints have microbial abundances comparable to starting material. There were two ASVs identified at ≥5% relative abundance across all samples. An ASV from the genus *Streptomyces* at 25.1% average relative abundance across all samples, and from the genus *Saccharopolyspora* at 53.2% average relative abundance across all samples. These affiliated more closely with oxic sample profiles than those of anoxic samples (Figure 3.8 B), despite *Saccharopolyspora* being more abundant in oxic low and medium water activities profiles compared to *Streptomyces*, which associated with high water activity sample profiles (Figure 3.8 A).

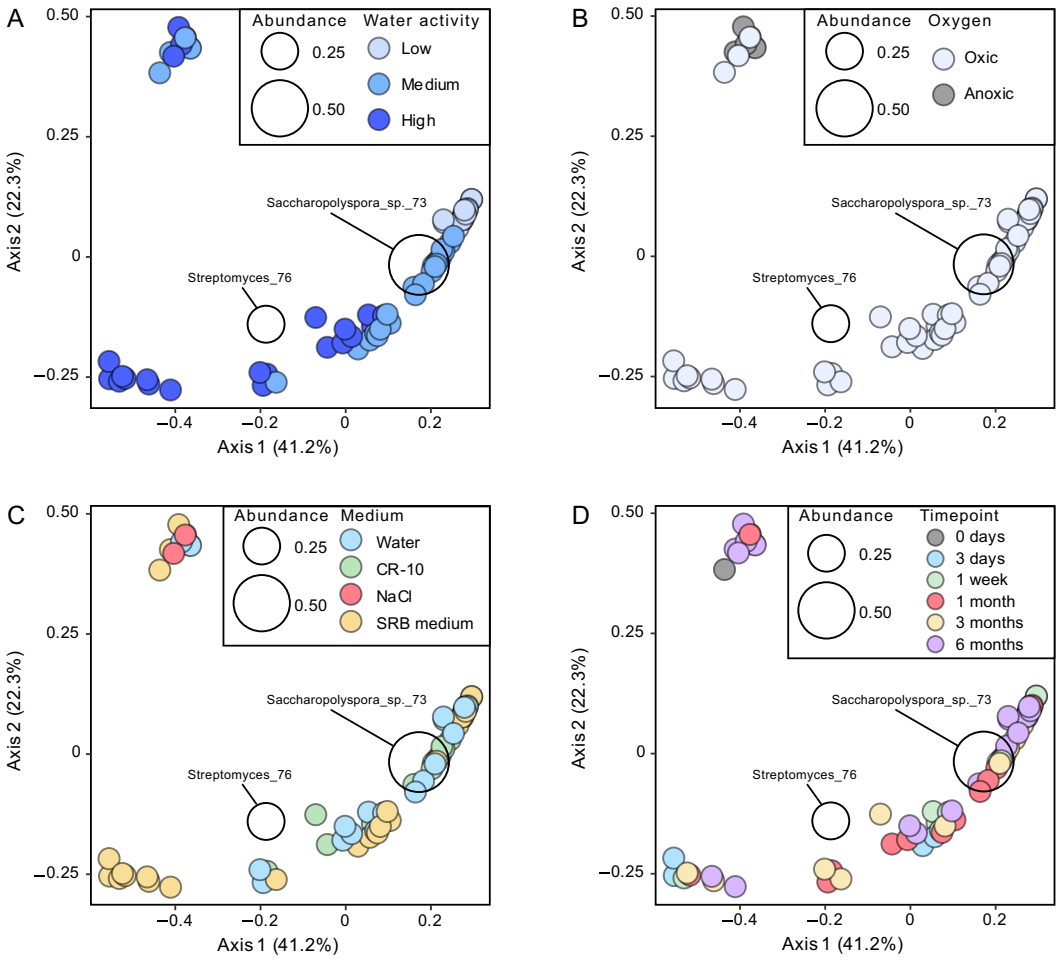


Figure 3.8. Principal coordinate analysis (PCoA) biplots using Bray-Curtis dissimilarity distances comparing microbial community profiles based on A) water activity, B) oxygen condition, C) medium, and D) timepoint across samples. Samples were rarefied to 2040 reads. Genera displayed are ≥ 5% relative abundance across all samples and are positioned in ordination based on correlation of taxon abundance within individual sample profiles.

Analysis of 16S rRNA gene profiles displaying ASVs that are ≥15% relative abundance in oxic microcosm samples identified six bacterial phyla, with ASVs affiliated with *Actinobacteriota, Firmicutes,* and *Proteobacteria* accounting for the majority of ASVs, followed by *Chloroflexi, Bacteroidota,* and *Fusobacteroita* (Figure 3.9). The only archaeal ASVs present in all oxic sample profiles were from the *Nitrososphaeraceae* family in the *Crenarchaeota*, consisting of ammonia-oxidizing archaea, and had ≤27% relative abundance in sporadic samples, with an average of 10.6% across those samples. Oxic microcosms had a dominance of *Actinobacteriota* taxa*,* specifically of genera *Saccharopolyspora* and *Streptomyces* by the one-week timepoint in oxic microcosms hydrated with water, CR-10, or SRB medium. These three media always had similar profiles in oxic microcosms in comparison to microcosms hydrated with high-salinity medium. Sample replicates often displayed similar profiles, but showed more variety in lower biomass samples, such as early timepoints (day zero and day three) or samples hydrated with high-salinity medium. The *Actinobacteriota* phylum is known to consist of Gram-positive bacteria that are distributed across a variety of terrestrial and aquatic environments [114].

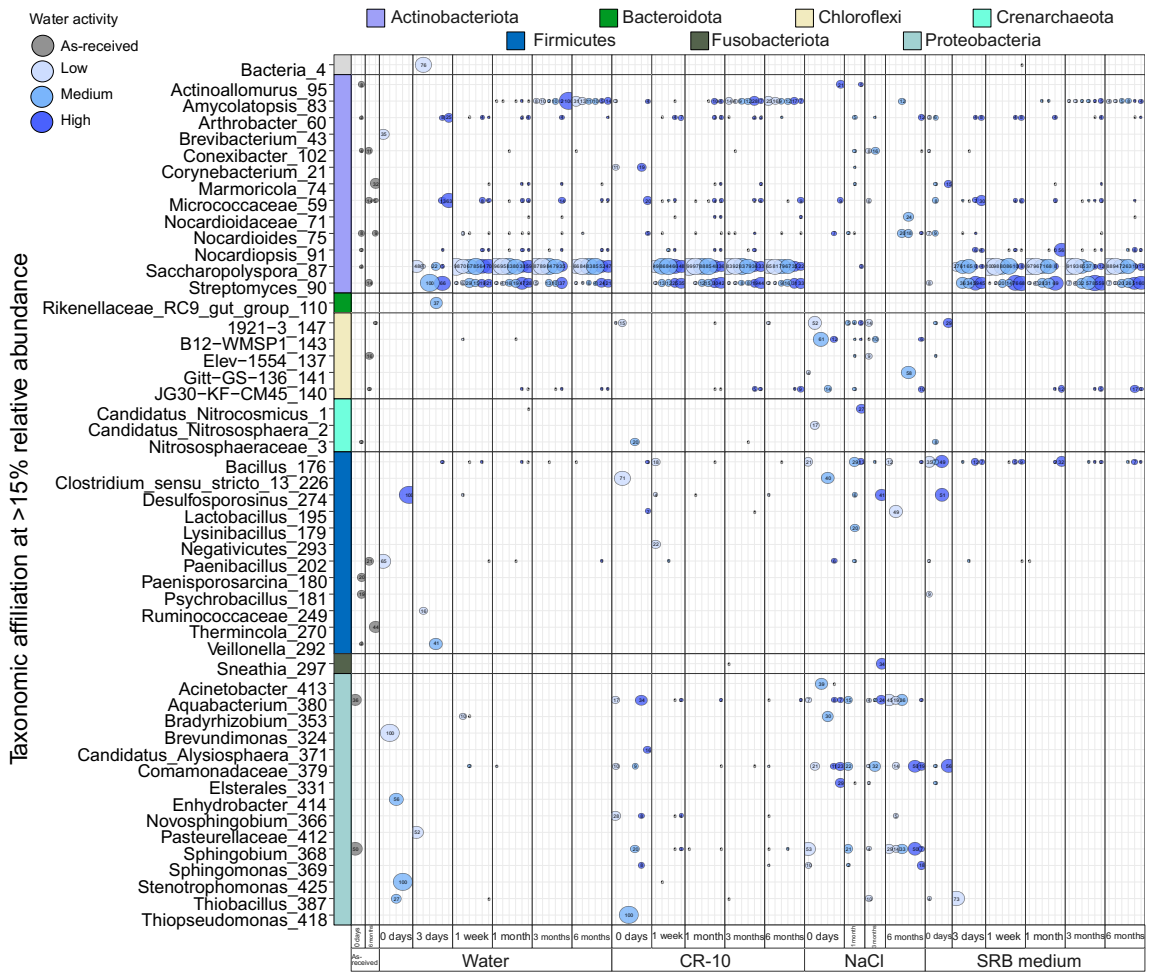


Figure 3.9. Bubble plot of the 16S rRNA gene profile of oxic microcosms across all sequenced timepoints. Taxa are collapsed to genus level. Only taxa ≥15% relative abundance in any given sample profile are displayed.

Saccharopolyspora are spore-forming, Gram-positive, non-motile bacteria, with the genus currently consisting of over 30 species, with the majority occupying soils, plants, and marine sediments [115]. In microcosm incubations, the ASV associated with *Saccharopolyspora* was enriched in samples associated with oxic conditions hydrated with water, CR-10, and SRB medium, although it had a lower average relative abundance in high water activity samples when present (30.9%) compared to medium and low water activities (73.6% in medium water activities and 80.3% in low water activities across all media; Figure 3.9). In samples hydrated with SRB medium, the relative abundance of *Saccharopolyspora* in high water activities was lower in comparison to water and CR-10 hydrated microcosms (≤15% when present). *Saccharopolyspora* has previously been identified as a dominant taxon in processed B36 bentonite clay hydrated with Opalinus clay pore-water solution in anoxic conditions as well as natural in calcium-magnesium bentonite compacted and kept in boreholes for two years [116, 117], but is not commonly reported as a dominant ASV in most bentonite research that includes compaction [24, 39, 45, 53, 118]. The *Streptomyces* genus was the second-most abundant ASV in oxic water, CR-10, and SRB medium-hydrated microcosms, having the highest average relative abundances in high water activities when present (43.8%) and the lowest average relative abundances in low water activities (3.3%). In high water activities, *Streptomyces* had overall higher relative abundances in samples hydrated with SRB medium in comparison to samples hydrated with water or CR-10. *Streptomyces* are spore-forming, aerobic, Gram-positive filamentous bacteria commonly found in soils, and are known for producing the antibiotic streptomycin, among others [119, 120]. *Streptomyces* has been found frequently in previous bentonite community composition analyses, including dry clay and borehole modules of compacted MX-80 bentonite in anoxic conditions [24, 73, 117].

After one-month of incubation with low, medium, and high water activities for samples hydrated with water, CR-10, and SRB medium, the genus *Amycolatopsis*, also belonging to the *Actinobacteriota* phylum, began to increase in relative abundance to an average of ~9% in 49 of 97 samples in which it was detected (Figure 3.9). This indicates that the community composition of samples may still experience shifts after initial establishment of dominant ASVs. Other actinobacterial genera frequently detected at low abundances in

high water activity sample profiles in samples hydrated with water, CR-10, or SRB medium include *Micrococcaceae* and *Arthrobacter*. Because *Actinobacteriota* are commonly spore-formers, the microorganisms present in these samples are most likely surviving in a state of desiccation and metabolic inactivity until favourable conditions are introduced, including an increase in water activity, and most likely use organic carbon within the microcosms [13, 20, 24, 73, 114, 117, 120].

Because the relative abundances of these dominant ASVs are increasing temporally, detection of these taxa is not being derived from relic DNA, but from viable organisms. It is also possible that the relative abundance of dominant ASVs is increasing due to other taxa dying off. At ≥15% relative abundance, ASVs affiliated with the genus *Bacillus* are detected at low relative abundances in samples hydrated with SRB medium (average of 10.1% in 17 of 33 samples in which it was detected) with most samples being from high water activities (Figure 3.9). *Bacillus* spp. have frequently been sequenced and cultivated as dominant taxa within MX-80 bentonite [20, 24], and likely favour high water availability while using organic material. Antibiotic-producing *Actinobacteriota* may be causing suppression of other microorganisms in samples dominated by these genera, however it has previously been suggested that sorption of naturally produced antibiotics in soils may cause a loss of antibacterial activity, especially in a clay matrix [67, 121–123]. It is possible that the *Bacillus* genus is not dominating 16S rRNA gene profiles due to competition with more abundant actinobacterial taxa.

At ≥15% relative abundance, sequenced oxic microcosm samples hydrated by the high-salinity medium revealed inconsistent profiles (Figure 3.9). *Saccharopolyspora* was only detected in one high-salinity medium and high water activity sample at 3% relative abundance and one sample at a low water activity at 8% relative abundance. Out of 18 samples, the highest average abundances seen most consistently for these microcosms were from ASVs affiliated with *Proteobacteria*, specifically from the genus *Aquabacterium* detected in 11 samples (15.4 ± 14.4% average relative abundance across water activities), from the family *Comamonadaceae* detected in nine samples (21.7 ± 13.4% average relative abundance across water activities), and from the genus *Sphingobium* detected in eight

samples (26.4 ± 18.4% average relative abundance across water activities). Although salt-tolerant denitrifying *Proteobacteria* have previously been identified in mud slurries [124], the three genera most abundant in high-salinity medium samples were most commonly found in soil or fresh water habitats [125–127]. Although their presence within high-salinity samples is unclear, both *Aquabacterium* and *Sphingobium* were detected in dry as-received MX-80 starting material at the zero-day timepoint at 36% and 50% relative abundance, respectively. This could indicate that these taxa are naturally present and surviving at low abundances in harsh conditions, and potentially do not proliferate within any other medium due to competition with actinobacterial taxa. This also suggests that high salinity conditions suppress growth of *Streptomyces* and *Saccharopolyspora*. The remaining community composition of samples hydrated with high-salinity medium reflects similarly inconsistent patterns seen for dry as-received MX-80 samples, indicating very low biomass and a lack of microbial proliferation within these microcosms, in agreement with cultivation data (Figure 3.4).

The community composition of taxa at ≥15% relative abundance in anoxic microcosms did not reveal any consistent patterns for any condition or timepoint (Figure 3.10). Detected ASVs affiliated with 11 phyla, with most originating from *Actinobacteriota, Firmicutes,* and *Proteobacteria*, and others from *Acidobacteroita, Bacteroidota, Bdellovibrionota, Chloroflexi, Cyanobacteria, Desulfobacterota, Fusobacteria, Planctomycetota*, and *Crenarchaeota*; the latter being the only archaeal taxa detected, from the *Nitrososphaeraceae* family. The contrast between the community profiles of oxic and anoxic microcosms reflects low 16S rRNA gene abundances and cultivation-based estimates from the same anoxic microcosms (Figure 3.5). A previous study suggested oxygen trapped within “anoxic” bentonite becomes bioavailable upon saturation, both yielding aerobic heterotrophic growth and inhibiting SRB growth [77]. However, the anoxic microcosm community profiles obtained here suggest no consistent proliferation of any microorganisms, which suggests that any residual oxygen cannot support aerobic growth within anoxic bentonite.

The *Streptomyces* genus dominant in oxic microcosms was seen in 14 out of 52 anoxic samples across all hydrated microcosms (Figure 3.10). However, abundance of this genus results from a different ASV affiliated with *Streptomyces* than the ASV dominant in oxic microcosm profiles. *Streptomyces* taxa have previously been identified in borehole samples kept under anoxic conditions [73], as well as as-received dry clay [24], and it was suggested that the detection of aerobic genera could be due to relic DNA absorbed in the bentonite matrix [61, 77]. Because there was no consistent microbial community profile for any anoxic microcosm timepoints and overall cultivation and 16S rRNA gene abundances did not increase over time, it may be that ASVs that were detected originate from dead or dormant cells, endospores, or extracellular DNA.

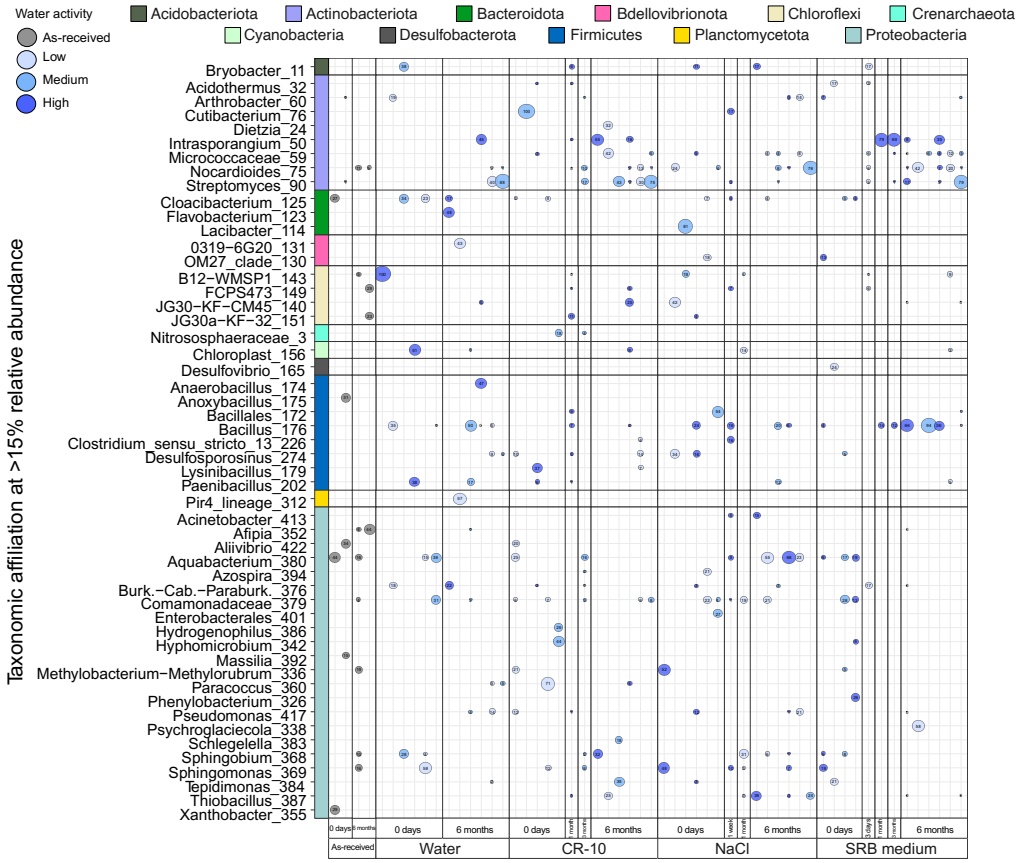


Figure 3.10. Bubble plot of the 16S rRNA gene profile of anoxic microcosms across all sequenced timepoints. Taxa collapsed to genus level. Only taxa ≥15% relative abundance in any given sample are displayed. "Burk.-Cab.-Paraburk." represents "Burkholderia-Caballeronia-Paraburkholderia".

Desulfosporosinus, a Gram-positive, spore-forming genus of SRB, has previously been detected in saturated bentonite and resulting cultures [24, 45, 73, 77, 97, 118, 128]. For all oxic and anoxic microcosms, this genus was detected at an average of 11.9% relative abundance in 8 out of 58 anoxic samples across all water activities and media, and at an average of 25.5% relative abundance in 8 out of 123 oxic samples across all water activities and media. Taxa affiliated with *Desulfosporosinus* were not previously detected at high abundances in dry MX-80 clays [24], and there were no ASVs affiliated with this genus detected in any as-received MX-80 materials in this experiment. These SRB may be surviving in the bentonite as spores that are difficult to lyse during DNA extraction, although again it is unclear why there was no proliferation seen for anoxic microcosms, specifically in samples hydrated with SRB medium at high water activities, especially considering that *Desulfosporosinus* typically metabolize lactate, a component of the SRB medium used in this research [29, 30, 118]. The detection of this SRB in microcosm samples can be attributed to the presence of spores or relic DNA in the bentonite, and indicates that even in favourable conditions, there may be factors preventing SRB proliferation. The lack of SRB growth seen in this experiment will most likely be increased with the addition of pressure in a DGR environment.

3.3.3. Indicator species identified across microcosm parameters

An indicator species analysis identified 12 ASVs that were most strongly associated with hydrated oxic microcosm samples (Table 3.1; Figure 3.11). Out of the four different media tested in this study, water, CR-10, and SRB medium had the same indicator ASVs and were grouped together via multi-level pattern analyses, being affiliated with *Saccharopolyspora* and *Streptomyces*, both with associations >0.40. The *Streptomyces* ASV was also determined as an indicator in a high and medium water activity grouping (association of 0.47), and *Saccharopolyspora* was determined as an indicator in a low and medium water activity grouping (association of 0.38).

Table 3.1. Indicator ASVs and strength associations as determined by an indicator species analysis for all media and water activities in hydrated oxic microcosms.

Parameter	Sample type	Indicator ASV	Phylum	Indicator value	*p* value
Medium	Water + CR-10 + SRB medium	Saccharopolyspora_sp._9	*Actinobacteriota*	0.42	0.02
		Streptomyces_8		0.41	0.02
	NaCl	Comamonadaceae_10	*Proteobacteria*	0.42	0.01
		Aquabacterium_11		0.37	0.03
		Sphingobium_12		0.28	0.03
Water activity	High	Arthrobacter_1	*Actinobacteriota*	0.53	0.01
		Micrococcaceae_2		0.42	0.02
		Nocardiopsis_3		0.41	0.02
		Micrococcaceae_4		0.34	0.04
		Paracoccus_5	*Proteobacteria*	0.22	0.05
		JG30-KF-CM45_6	*Chloroflexi*	0.19	0.03
	High + medium	Streptomyces_8	*Actinobacteriota*	0.47	0.02
	Low + medium	Saccharopolyspora_sp._9	*Actinobacteriota*	0.38	0.04
	Low	Saccharopolyspora_sp._7	*Actinobacteriota*	0.22	0.04

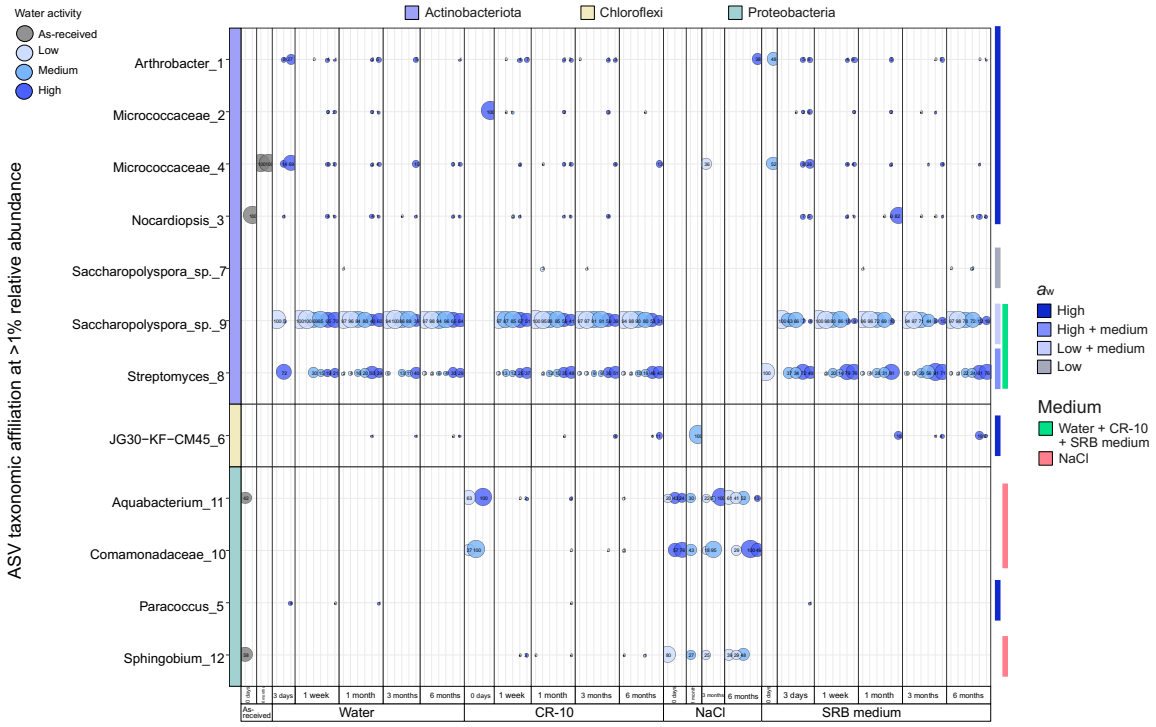


Figure 3.11. Bubble plot of the 16S rRNA gene profiles of ASVs in oxic microcosms that were identified by an indicator species analysis where p <0.05. Taxa are colour coded by bars (on right) representing the corresponding parameters they are associated with. Only taxa ≥1% relative abundance in any given sample are displayed.

The strongest associations for indicator ASVs in the water, CR-10, and SRB medium group as well as all groupings of water activity were from *Actinobacteriota* (Table 3.1). In samples hydrated with high-salinity medium, only genera *Sphingobium*, *Aquabacterium*, and *Comamonadaceae* from the *Proteobacteria* phylum were identified. The ASV affiliated with *Saccharopolyspora* associated with water, CR-10, SRB medium, and low and medium water activity treatments had no detection in day-zero timepoints, or in any high-salinity medium samples. At relative abundances ≥1% of all indicator ASVs, *Saccharopolyspora* was more abundant in low water activities than in medium water activities (Figure 3.11). In high water activities, *Saccharopolyspora* had a much lower average relative abundance in microcosms hydrated with SRB medium than in microcosms hydrated to a high water activity with water or CR-10. The ASV affiliated with *Streptomyces* associated with water, CR-10, SRB medium, and medium and high water activity microcosms had a low relative abundance in low water activities over time. The average relative abundance of *Streptomyces* in medium water activity samples was higher in SRB medium-hydrated microcosms than in microcosms hydrated to a medium water activity with water or CR-10. Because these ASVs were not detected in microcosms hydrated with high-salinity medium and were infrequently detected in early timepoints (zero and three-days), it is likely that the identified indicator species are viable microorganisms that establish over time in oxic microcosms and are not dominant in as-received MX-80 bentonite clay.

The two ASVs identified as indicator species affiliated with *Saccharopolyspora* and *Streptomyces* were the only indicator organisms connected across parameters. In sequenced oxic microcosm samples hydrated with water, CR-10, or SRB medium from the one-week to six-month timepoint, there was a negative linear relationship between relative abundances of the *Saccharopolyspora* ASV and water activity ($R^2 = 0.62$) and a positive relationship between relative abundances of the *Streptomyces* ASV and water activity ($R^2 = 0.53$; Figure 3.12). This corresponds to trends seen in the bubble plot of indicator ASVs ≥1% relative abundance in oxic microcosms (Figure 3.11).

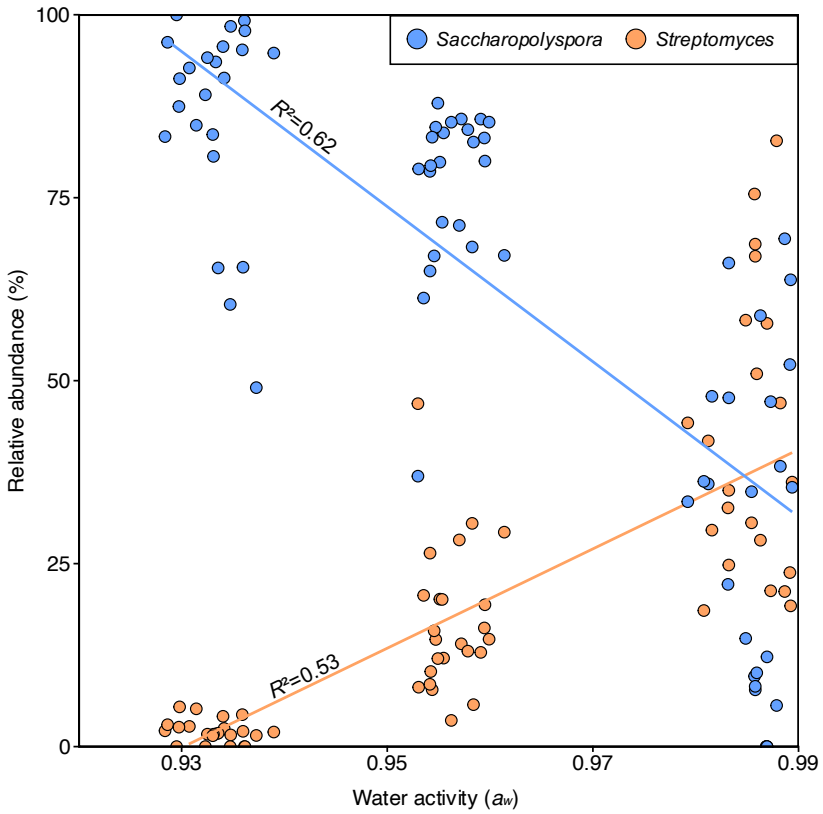


Figure 3.12. Relative abundances of identified indicator ASVs affiliated with *Saccharopolyspora* and *Streptomyces* compared to raw water activity measurements of all sequenced samples from oxic microcosms hydrated with water, CR-10, or SRB medium from the one-week timepoint onward. R^2 = 0.62 for the *Saccharopolyspora* ASV (blue), R^2= 0.53 for the *Streptomyces* ASV (orange).

Saccharopolyspora and *Streptomyces* are both found within the *Actinomycetales* order. *Saccharopolyspora* species have been isolated from a range of environments, from soils (*S. antimicrobica*), a hypersaline lake (halophilic *S. halotolerans*), and from Saharan soil (halophilic *S. ghardaiensis*) [129–131]. Because this genus is often found in arid or saline environments, it is possible that there is an adaptation to low water activities, allowing for proliferation in environments that may be unfavourable for other microorganisms. It is possible that this explains why the ASV representing the *Saccharopolyspora* genus was more abundant in low and medium water activity microcosm profiles. *Streptomyces* taxa are common soil bacteria, but they are also often found in water reservoirs, and a previous study

identified that the beta-lactam antibiotic production of *S. clavuligerus* is sensitive to water activity, decreasing rapidly after $a_w < 0.997$, whereas growth decreased by 88% at a_w 0.986 [132, 133]. These data demonstrate water-activity preferences of taxa affiliated with this bentonite-associated genus and can potentially be useful for predicting outcomes of future DGR-related experiments.

3.4. Application to DGR research

Both ASVs affiliated with *Saccharopolyspora* and *Streptomyces* indicator species for oxic water, CR-10, and SRB medium hydrated microcosms have been found in oxic pressure vessel experiments saturating MX-80 bentonite (as HCB or GFM) to different dry densities. The indicator *Streptomyces*-affiliated ASV was detected in 28 out of 72 GFM pressure vessel samples with an average relative abundance of 20.5% across dry densities, and was a dominant ASV in samples saturated to 1.25 g/cm^3 dry density compared to 1.6 g/cm^3 [Beaver, 2023 (unpublished)]. This ASV was less prevalent in pressure vessels packed with HCB and was detected in 19 out of 135 samples at an average relative abundance of 2.3%. The *Saccharopolyspora* ASV was not detected in any GFM pressure vessel samples and was only found at 0.2% relative abundance in one of 135 HCB samples [Beaver, 2023 (unpublished)]. The overall dominant ASVs detected in all pressure vessel samples were affiliated with *Pseudomonas* and *Bacillus* [Beaver, 2023 (unpublished)], which have previously been detected at high abundances in compacted clay and starting material bentonite and associated cultures [20, 24, 39, 45, 53, 134]. Although this project used a different batch of MX-80 than was used in previous pressure vessel experiments, comparing the hydrated microcosms in this project to bentonite samples kept under pressure may suggest different microbial community responses. Throughout the DGR lifetime, it is possible that as conditions shift during the phases before equilibrium, different microbial communities will dominate.

The lack of microbial proliferation based on cultivation, nucleic acid abundance, and community profiles in anoxic microcosms suggests that once a DGR reaches anoxic conditions within a few weeks to ~50 years after repository closure [14, 17], abundant microbial proliferation will cease even in the absence of pressure as a factor of suppression,

unless there is bioavailable oxygen adsorbed in the bentonite matrix for microbial use as previously suggested [77]. Additionally, groundwater composition will affect microbial community composition of the bentonite in oxic conditions, as seen in comparisons of microcosms hydrated with CR-10 and high-salinity medium. The crystalline rock bed groundwater composition is considered low-salinity [13], and a low salinity level does not appear to suppress microbial abundances or alter community profiles in microcosms when compared to hydration with water. A high-salinity hydration medium in bentonite may prevent microbial proliferation based on the TDS content alone, as the water activity is not conducive to microbial viability and does not appear establish a community over time. However, the possibility of a halotolerant microbial community already established within these groundwater sites cannot be ruled out. It can also be presumed that the water activity previously thought to suppress microbial proliferation in bentonite ($a_w < 0.96$) [13] must be coupled with pressure to suppress microbial culturability to that of starting material. Although overall cultivation abundances in low water activities in uncompacted microcosms were lower, a water activity of 0.93 still allowed microbial proliferation in bentonite (Figure 3.4), and community profile analyses display that certain ASVs may prefer such conditions (*Saccharopolyspora*; Figure 3.9).

3.5 Large-scale microcosms

Twelve oxic large-scale microcosms were produced by scaling up the bentonite mass used in original small-scale microcosms ten-fold. These were hydrated with water to a low or high water activity, and were processed using the same methods as small-scale microcosm analyses at zero-day, one-week, and one-month timepoints. Samples from the large-scale microcosms will be analyzed for PLFA abundance data as well as NOM profiles, which require more mass than available in small-scale microcosms, hence the reproduction and scaling-up of select microcosm conditions. These complementary techniques will provide additional measures of microbial abundance and community composition, without interference from relic DNA in the bentonite matrix, and will also give insight as to which substrates are potentially being used by microorganisms in the bentonite over time [24, 73, 79]. Although complementary PLFA and NOM data have not yet been produced, the production of large-scale microcosms provides an opportunity to compare data to small-scale

microcosms produced in similar conditions and assess the reproducibility of microcosm experiments using different masses of bentonite.

Water activity data (Figure 3.2, Figure 3.13), abundances (Figure 3.4, Figure 3.14), and community profiles (Figure 3.9, Figure 3.15) revealed reproducibility between large-scale and small-scale microcosm experiments produced using similar conditions at each tested timepoint. Across all timepoints and water activities, the average water activity and moisture contents did not change when comparing small-scale and large-scale experiments at the same timepoints (Mann-Whitney U test, $p > 0.05$; Figure 3.13).

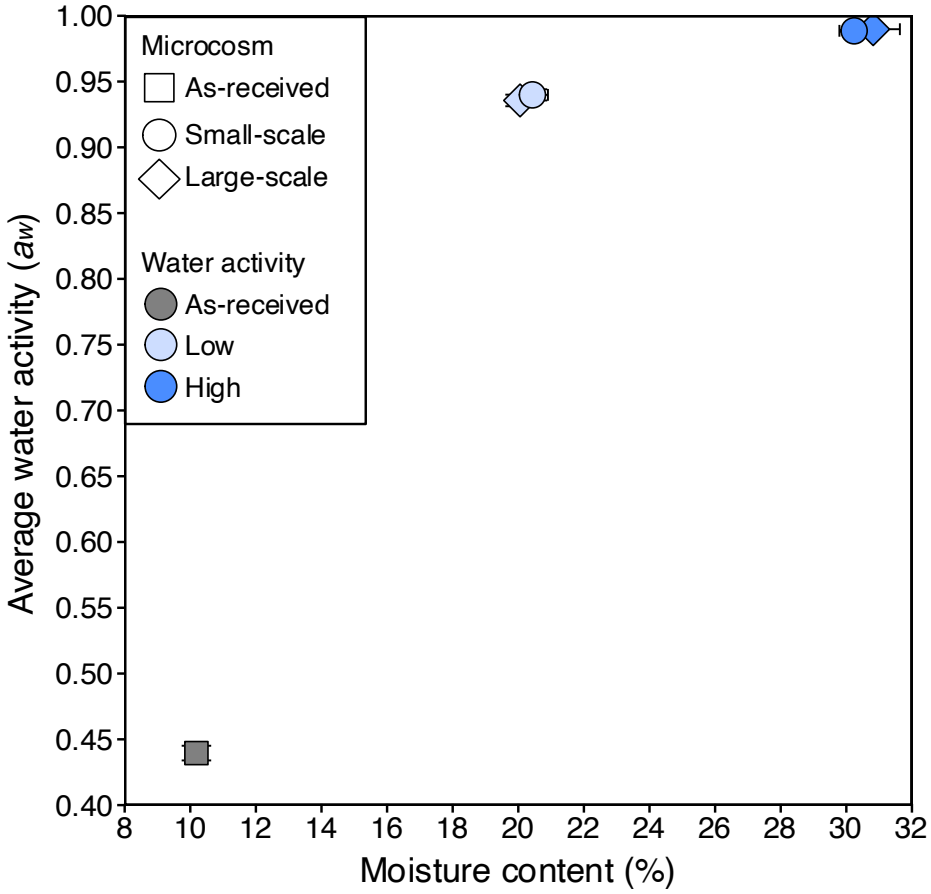


Figure 3.13. Average water activity and moisture content measurements in small-scale and large-scale microcosms at targeted water activities. Each point is based on 12 samples, including all timepoints and duplicate microcosms. Error bars represent the standard deviation between all readings across all microcosms and timepoints.

Abundance data of 16S rRNA gene copy data, as well as culturable heterotrophs and SRB reveals comparable trends across small-scale and large-scale microcosms (Figure 3.14). The large-scale microcosms reveal a higher average abundance in low water activity microcosms by the one-week timepoint compared to the small-scale microcosms, however large confidence intervals display a range of uncertainty, and heterogeneity within bentonite samples might account for this variation. High water activity microcosms are similar by the one-week timepoint between both large-scale and small-scale microcosms. Culturable aerobic heterotrophs for both large and small-scale microcosms showed a significant increase in abundance in high water activity microcosms by the one-week timepoint. Culturable anaerobic heterotrophs remained below the lower limit of quantification (2.5×10^3 CFU/gdw) or had no detectable growth in large-scale microcosms. Culturable SRB remained unchanged over time in all tested conditions.

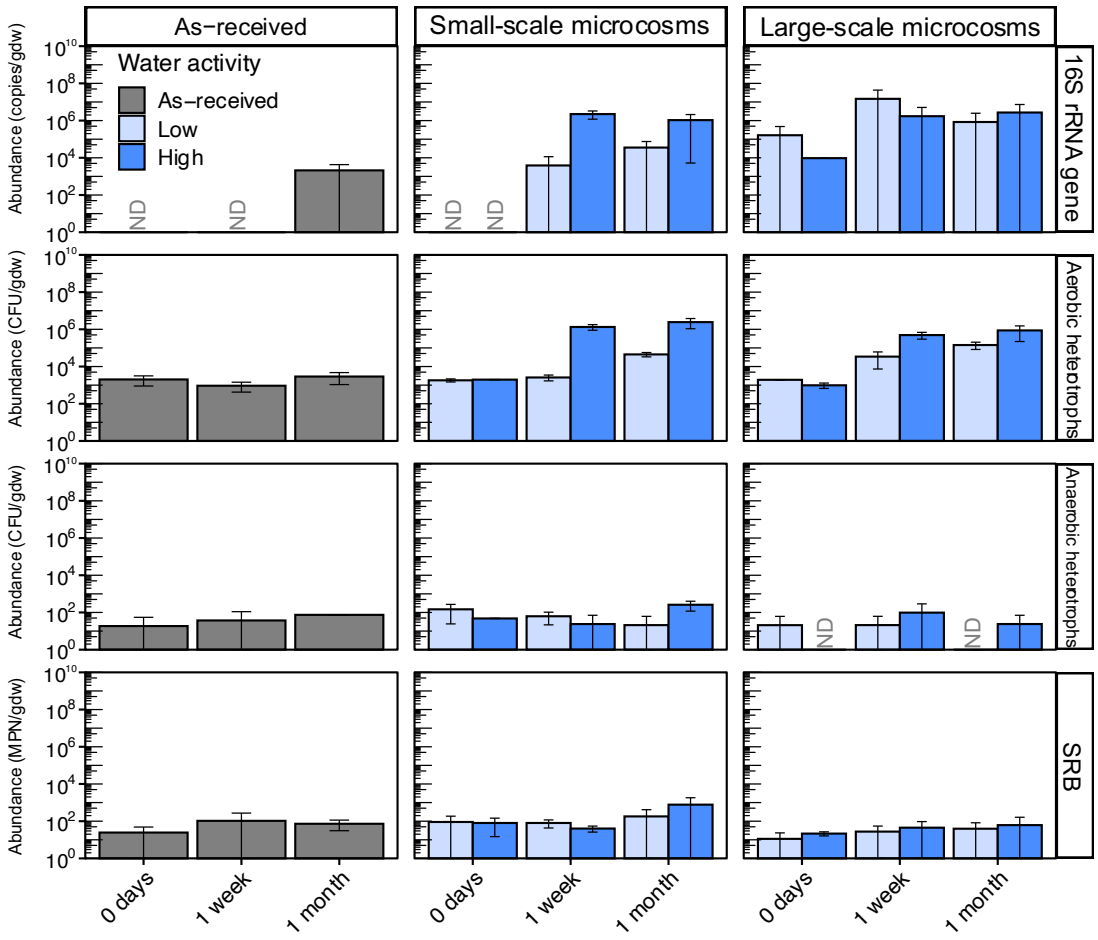


Figure 3.14. Average abundances of the 16S rRNA gene (copies/gdw), aerobic heterotrophs (CFU/gdw), anaerobic heterotrophs (CFU/gdw), and SRB (MPN/gdw) from as-received clay or hydrated large-scale or small-scale microcosms at low or high water activities over time. Error bars represent 95% confidence intervals between the average of biological replicates. The lower limit of quantification (background level) for heterotrophs is 2.5 x 10^3 CFU/gdw. No detectable amplification or growth is indicated by "ND".

Community profiles showing ASVs ≥15% relative abundance comparing the 16S rRNA gene in small-scale microcosms (Figure 3.9) to large-scale microcosms (Figure 3.15) revealed similar predominant *Actinobacteriota*, specifically ASVs affiliated with *Saccharopolyspora* and *Streptomyces*, as seen in oxic small-scale microcosms hydrated with water, CR-10, or SRB medium. Profiles from zero-day timepoints had inconsistent ASV relative abundance profiles, similar to those observed for as-received starting material. The *Saccharopolyspora* genus had an average relative abundance of 94.3% in low water activities across both small-scale and large-scale microcosms and was detected in all hydrated samples after the zero-day timepoint (Figure 3.15). For high water activities, this genus had a lower relative abundance at 46.7% and was detected in all hydrated samples after the zero-day timepoint, as well as one zero-day timepoint sample at a relative abundance of 8%. The *Streptomyces* genus had the highest relative abundance in samples hydrated to high water activities with an average of 20.6% across all small-scale and large-scale microcosms and was detected in all hydrated samples after the zero-day timepoint, as well as one zero-day timepoint sample at a relative abundance of 2%, whereas low water activities had an average of 2.7% in 6 of 8 hydrated samples past the zero-day timepoint. In high water activity samples, *Micrococcaceae* is also present in low relative abundances.

The comparable community composition data from large-scale and small-scale microcosms indicates reproducibility for these microcosm experiments and the hydration techniques used to prepare the tested bentonite material. It is important to be able to reproduce experiments like this to continue testing potential conditions that will be experienced in a DGR environment. Being able to scale the mass of bentonite up while maintaining the same microbial abundance and composition patterns demonstrates the potential for accurate future large-scale microcosm experiments testing DGR conditions in the presence or absence of pressure. The addition of PLFA and NOM data, when available, will complement these results and provide a full-suite analysis on the microbial composition and potential metabolic activities within bentonite.

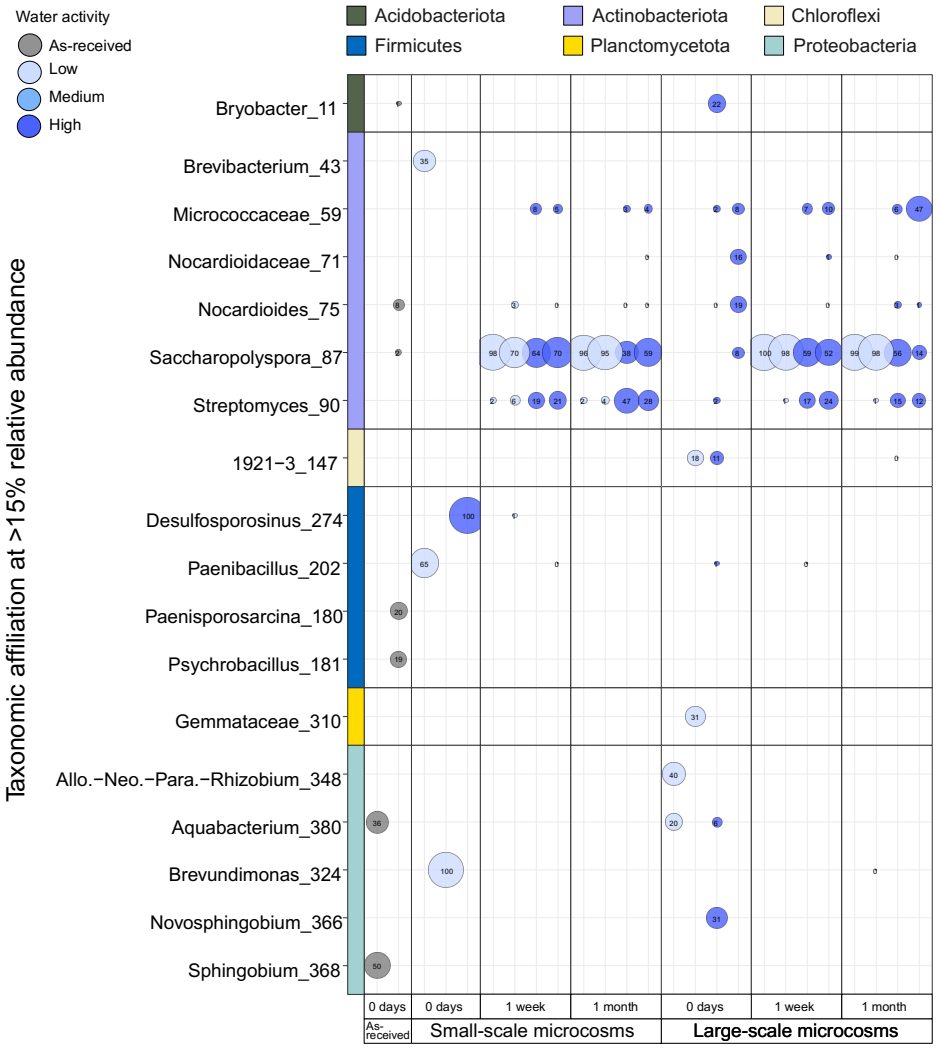


Figure 3.15. Bubble plot of the 16S rRNA gene profile of small-scale and large-scale microcosms across all timepoints. Taxa are collapsed to genus level. Only taxa ≥15% relative abundance in any given sample are displayed.

3.6 Comparison of community profile assays

One caveat to using cultivation data as a measure of abundance in bentonite clay is the discrepancy between 16S rRNA gene profiles from clay material versus resulting cultures. A previous study comparing nucleic acid profiles and cultured microorganisms from dry clays found that the two microbial compositions were inconsistent [24]. Similarly, in the current study, DNA sequences from swabs from cultivated R2A plates and pellets from MPN tubes from oxic microcosms hydrated with water or SRB medium up to the three-month timepoint did not correspond with sequencing data of the microcosm bentonite (Figure 3.16). Profiles from anoxic R2A plates and oxic R2A plates were similar to each other and were dominated by *Firmicutes*, specifically ASVs affiliated with the genus *Bacillus* across all conditions (Figure 3.17). From cultures in SRB medium, ASVs affiliated with *Firmicutes* were also dominant, and ASVs corresponding to the *Desulfosporosinus* genus had the highest relative abundances, followed by *Bacillus* and *Pelosinus* (Figure 3.18). Certain ASVs affiliated with genera seen in direct clay profiles, such as *Micrococcaceae* and *Streptomyces*, are present in R2A plate cultures, but do not reflect trends seen directly in microcosms (i.e., low relative abundance of *Streptomyces* in culture profiles; Figure 3.9). These data suggest that what is most abundant within the microcosms may not be accurately cultured from the clay, perhaps due to incorrect culturing conditions within a laboratory environment, or simply because the dominant ASVs are viable but non-culturable microorganisms [13, 24].

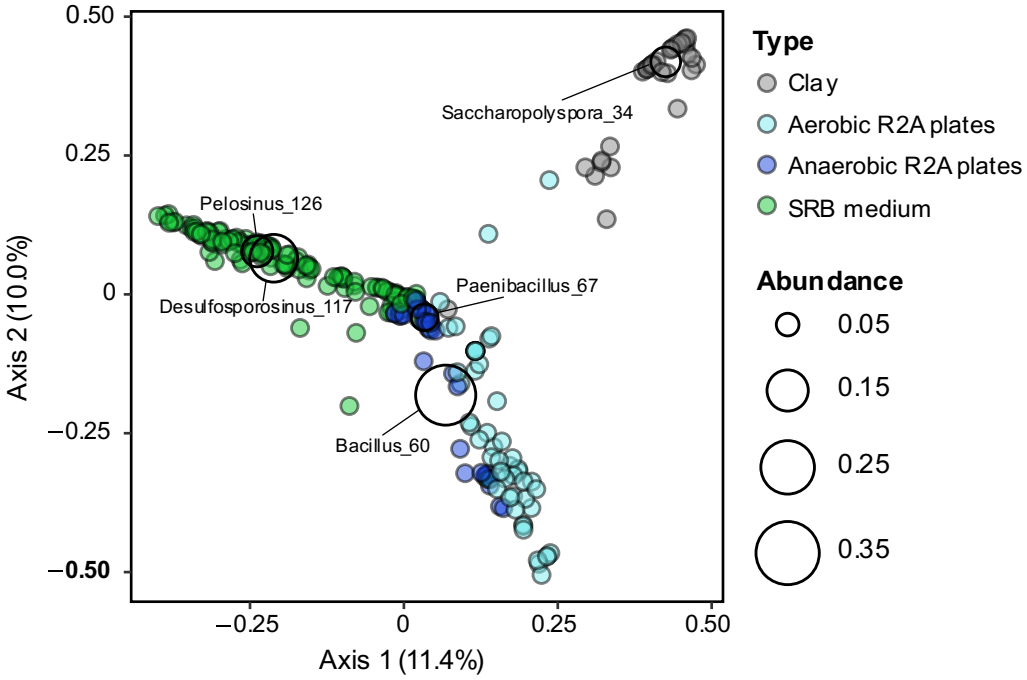


Figure 3.16. Principal coordinate analysis (PCoA) biplot using Bray-Curtis dissimilarity distances comparing 16S rRNA gene sequencing data of clays versus cultures derived from the clay. Samples were rarefied to 3000 reads. Genera displayed are ≥ 5% relative abundance and are placed based on associations of that taxon to samples.

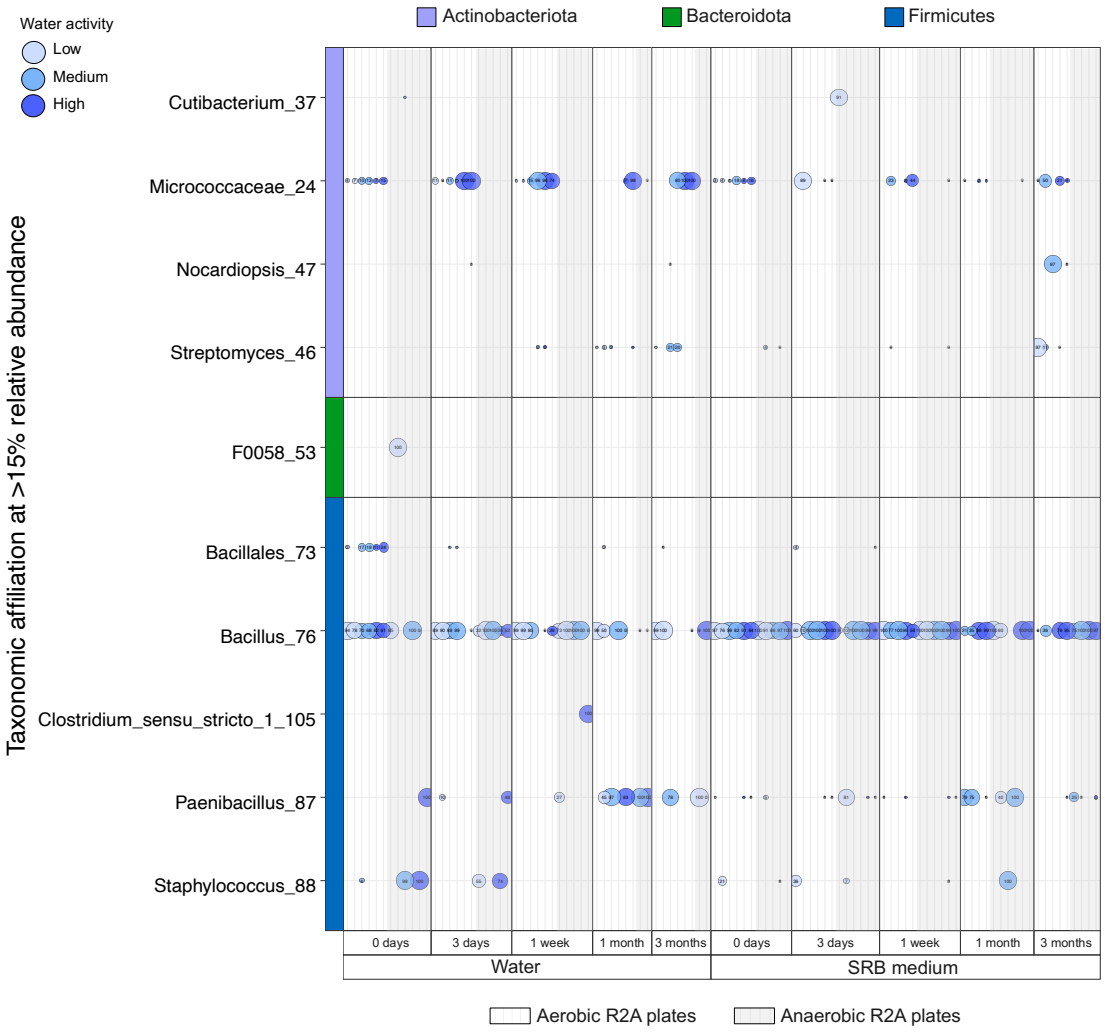


Figure 3.17. Bubble plot of the 16S rRNA gene profiles of ASVs from oxic and anoxic R2A plates inoculated from oxic microcosms hydrated with water or SRB medium up to the three-month timepoint. Taxa are collapsed to genus level. Only taxa ≥15% relative abundance in any given sample are displayed.

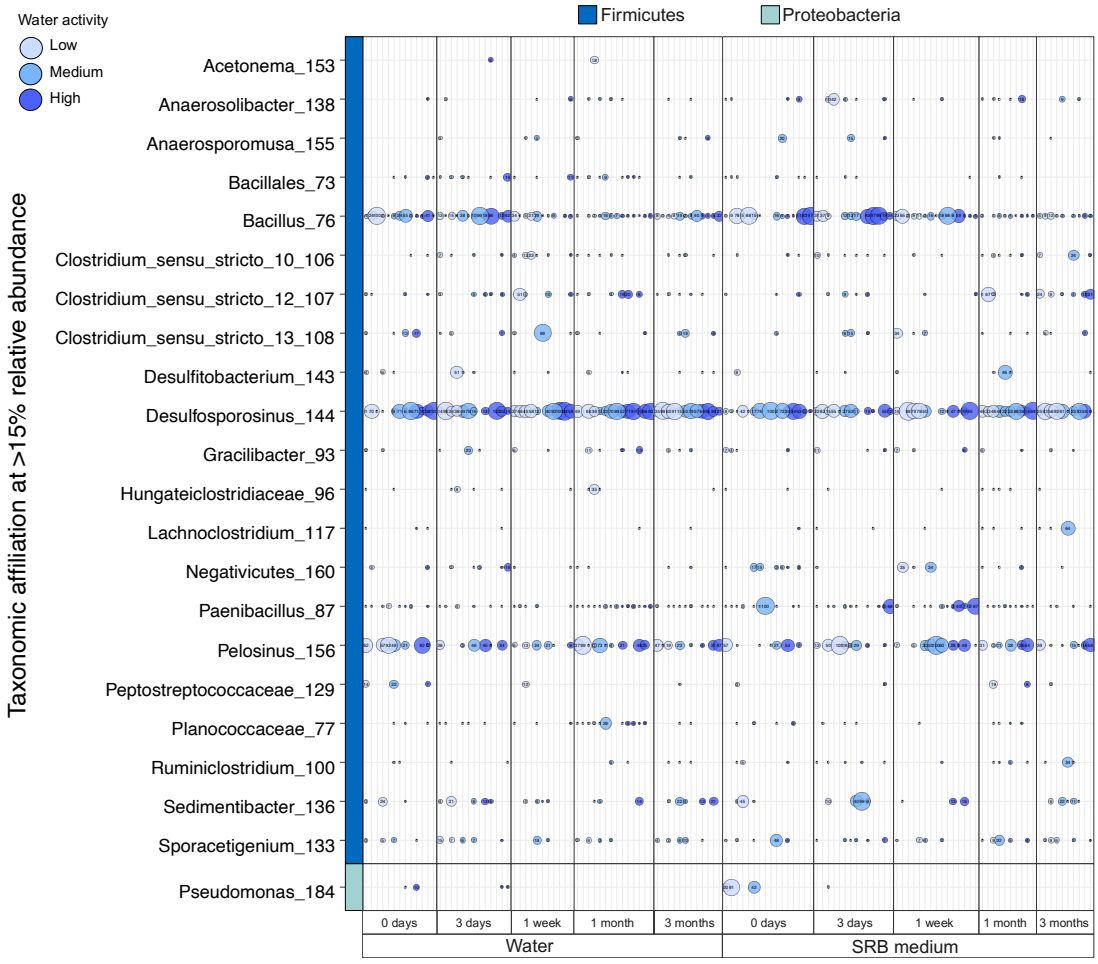


Figure 3.18. Bubble plot of the 16S rRNA gene profiles of ASVs from SRB medium inoculated from oxic microcosms hydrated with water or SRB medium up to the three-month timepoint. Taxa are collapsed to genus level. Only taxa ≥15% relative abundance in any given sample are displayed.

Bacillus-affiliated ASVs were previously reported dominant in heterotrophic cultures from a variety of dry bentonites, and *Desulfosporosinus* and *Bacillus* showed dominance in SRB cultures from these dry clays as well [24]. It appears that resulting cultures are not heavily influenced by the water activity of hydrated bentonite, although a water-activity-dependent community composition shift is seen in direct clay DNA profiles (Figure 3.9).

The oxic R2A plates revealed distinct colony morphologies on several plates, with many being large, fuzzy, dark green colonies mostly seen in cultures from microcosms hydrated with SRB medium after the one-week timepoint (Figure 3.19 A), as well as small, hard punctiform colonies (Figure 3.19 B). *Actinobacteriota*, specifically *Streptomyces*, are known to possess similar characteristics as fungi, including the production of mycelia [114, 119], and are known to produce a range of colony morphologies, including conidia similar to fungi or colonies that firmly adhere to agar [135]. It is possible that certain *Actinobacteriota* were being cultured, but due to the nature of their colony morphologies were not collected adequately for sequencing. However, this does not account for the discrepancy in the high abundance of ASVs affiliated with *Bacillus* and *Desulfosporosinus* in cultures compared to low abundance in clay nucleic acid profiles, and therefore suggests that cultivation-dependent methods are not capturing what is most abundant within bentonite samples.

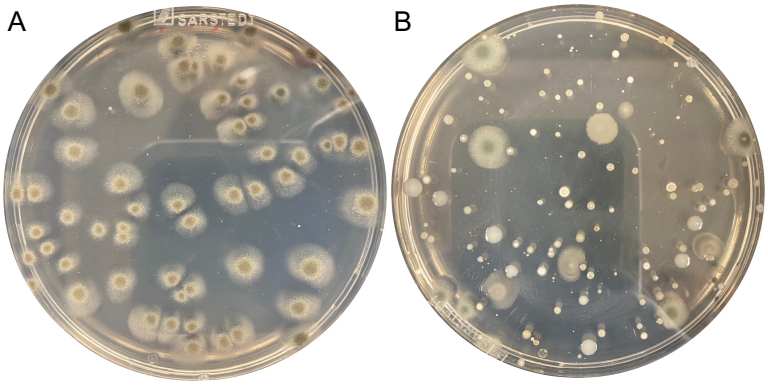


Figure 3.19. Images of oxic R2A plates associated with oxic microcosms hydrated with SRB medium to a A) medium water activity or B) high water activity cultivated at the three-month timepoint as representative examples of the presence of large, fuzzy, dark green colonies and small, hard, punctiform colonies.

Due to the presence of large, fuzzy, dark green colonies on certain oxic R2A plates (Figure 3.19), qPCR was carried out to quantify fungal 18S rRNA genes from DNA extracts from oxic microcosm samples hydrated with water or SRB medium up to the three-month timepoint to determine the potential presence of fungi (Figure 3.20). In oxic microcosms hydrated with water, fungi were detected at low abundances overall, and significantly increased by an order of magnitude in high water activities only at the one-week timepoint. In oxic microcosms hydrated with SRB medium, fungi were detected at a higher abundance than in water-hydrated microcosms, increasing in abundance by several orders of magnitude in high water activities by the three-day timepoint, and in low and medium water activities by the one-week timepoint. Overall, fungal abundances remained lower than prokaryotic abundances from the same microcosm samples as determined by 16S rRNA gene quantification (Figure 3.4). Fungi can often grow in lower water activities than most bacteria tolerate, and is likely that the increased presence of organic carbon in the SRB medium drove fungal proliferation [48, 136]. Fungi in bentonite have not been studied extensively, but fungi have nonetheless been detected in the subsurface, and a previous study found partly preserved filamentous fungal structures over 700 m deep in crystalline rock environments presumed to be anoxic [60, 136]. Fungal metabolisms producing H_2, CO_2, or organic compounds can also be coupled to sulfate reduction and fungi can form consortia with SRB [60, 136]. The fungal quantification data presented in this thesis indicate the potential presence of fungi within bentonite samples, and the potential for certain aerobic heterotroph abundance counts to also include fungal quantification. Future experiments would be helpful to quantify and sequence the 18S rRNA genes in a variety of hydrated bentonite samples, assess fungal community composition, and predict potential impacts fungi may have in these clays (e.g., use of available oxygen and NOM).

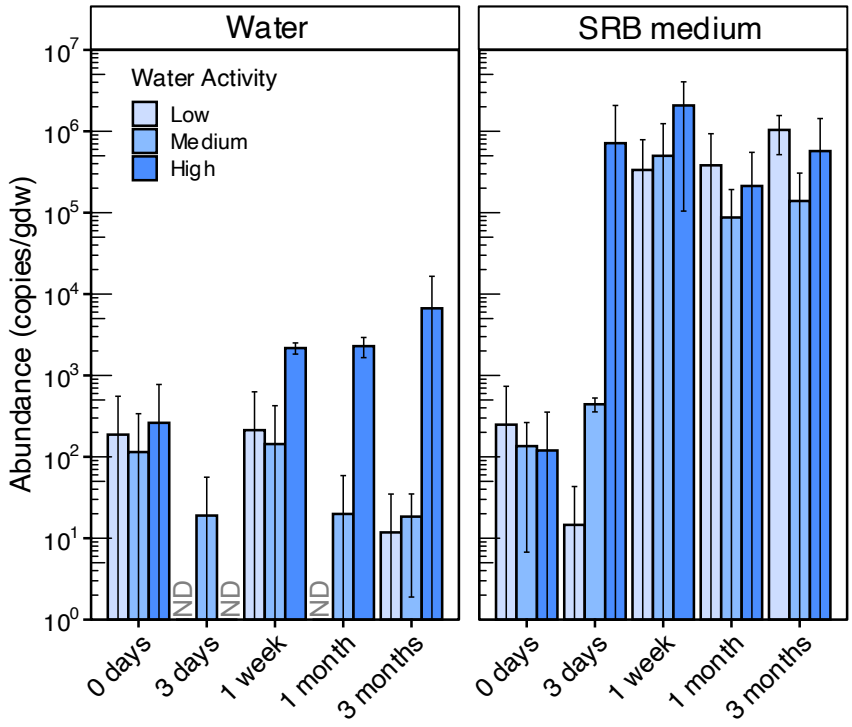


Figure 3.20. Average abundance of the 18S rRNA genes (copies/gdw), from oxic microcosm samples hydrated with water or SRB medium up to the three-month timepoint to determine the potential presence of fungi. Error bars represent 95% confidence intervals for the averages of biological replicates. No detectable amplification is indicated by "ND".

Differences in community composition profiles based on sequencing of cultures compared to sequencing of clay sample DNA extracts highlight the importance of using multiple techniques to study microbial populations associated with bentonite clay. Cultivation methods offer a direct measure of viability, nucleic acids capture live and dead cell DNA without cultivation bias, and qPCR offers abundance data for nucleic acids associated with all samples. Culturing and qPCR data together complement one another because qPCR data can quantify microorganisms that are not detected by cultivation and cultivation provides a better sense of microbial viability because PCR approaches detect relic DNA as well as DNA from viable cells. Additional approaches, such as collecting PLFA and NOM data, or using viability-based techniques such as ATP or PMA assays, would provide even more insight into the microbiology of bentonite clay.

Chapter 4
Conclusion and future directions

Canada's design for the proposed used nuclear storage solution consisting of a multi-barrier system 500-800 metres belowground must be extensively researched before implementation. This includes exploring the potential for microbiologically influenced corrosion occurring through the metabolism of SRB converting naturally occurring sulfates into hydrogen sulfide that can go on to corrode the copper-coating on used fuel containers. It is important to study which conditions in bentonite must be maintained to suppress microbial growth.

The main findings of this research demonstrate an association between increasing water activity and microbial proliferation, and show that low water activity alone is insufficient to prevent microbial growth. Specifically, there was water-activity-dependent actinobacterial growth seen in oxic conditions. A lack of microbial growth was seen in the presence of high salinity. In anoxic conditions, microbial proliferation did not occur. In all tested conditions in this research, SRB did not proliferate and were not present at high abundances in 16S rRNA gene sequences recovered directly from bentonite samples.

Together, abundance data as well as nucleic acid profiles of microcosm community compositions indicate that there is a preference for oxic conditions by microorganisms in the bentonite, and proliferation occurs at all water activity levels assessed, although there was water-activity-dependent actinobacterial growth detected. Although viability and growth were observed in all water activities assessed, the addition of pressure within a DGR may provide additional inhibitory factors on the microbial community, as shown in previous and concurrent pressure vessel-type studies. It is therefore imperative that there are multiple parameters working in combination to inhibit microbial growth in a DGR environment.

The data presented in this project suggest microbial suppression in high-salinity environments as well as anoxic environments, even without the additional factor of pressure. The DGR is presumed to achieve anoxic conditions shortly after closure, and this could

indicate that there will be a large decrease in microbial activity once those conditions arise. Additionally, should a high-salinity groundwater site be selected for DGR emplacement, it is likely that the groundwater composition is too saline for proliferation of microorganisms from bentonite due to the amount of TDS interfering with water availability, and this too should suppress microbial viability and proliferation even in the absence of pressure. However, these groundwater sites may contain naturally occurring microbial communities that have adapted to high salinity environments. In low-salinity conditions, microbial suppression may not be achieved by a low water activity alone, and additional factors of suppression such as pressure and anoxic conditions may be needed. The incorporation of elevated pressure (i.e., compaction and swelling) into the DGR system should contribute additional measures to prevent microbial proliferation, although swelling conditions will most likely not reach equilibrium until long after DGR closure. This research highlights the importance of studying a variety of suppression factors alone and in combination.

The data from microcosm experiments using hydrated MX-80 in the absence of pressure complement ongoing pressure vessel experiments compacting MX-80 to specific dry densities, and comparing the microbial profiles of these two methods indicates that communities contrast between environments with and without pressure. This suggests the community composition in MX-80 bentonite clay may shift depending on DGR conditions or bentonite starting material. The results of this research emphasize how variability within a DGR environment may impact microbial viability and community composition, and demonstrates the importance of researching all possible variations a DGR environment may experience before reaching a state of equilibrium.

Future research may take these data and apply the results to additional pressure vessel experiments, including inducing anoxic conditions as well as pressure and investigating how this affects microbial viability and abundance at different saturation levels. Using reference groundwater media to more accurately mimic how groundwater compositions, water activity, and pressure will affect the microbiology of MX-80 bentonite clay in DGR conditions is also recommended for pressure vessel experiments. Experiments investigating long-term effects on microbial viability, abundance, and community composition in these samples, in either the

presence or absence of pressure, are also recommended considering the longevity of a DGR system. Future research investigating the fungal community composition in similar samples (i.e., SRB medium-hydrated bentonite) would also be relevant considering the potential impact fungi could have on SRB proliferation if the production of fungal metabolites can be coupled with sulfate reduction in bentonite, although no increase in SRB abundance was detected in this study.

Because there is a potential cultivation bias seen when comparing 16S rRNA gene profiles from cultures versus direct bentonite samples, large-scale microcosm samples will be used in future assays to assess the PLFA representation within the bentonite and potentially distinguish only viable microorganisms. Additionally, large-scale microcosms will be used to analyze NOM profiles to track which substrates in the bentonite are being used up over time, potentially allowing a better understanding of the microbial metabolisms that are most common in these samples. Using the suite of methods including cultivation data, 16S rRNA gene abundances, nucleic acid profiles, PLFA analyses, and NOM profiles aims to provide a holistic investigation into the microbiology of bentonite clay and better inform the processes that may go on within a DGR environment. Additionally, future work should focus on establishing protocols to distinguish viable cells from extracellular DNA in bentonite, potentially including ATP or PMA assays.

This research explored a unique perspective on the microbiology of bentonite clay and DGR conditions without the impact of pressure to independently assess water activity and salinity as factors of microbial suppression. Low water activities in the DGR system are not intended to be the sole factor of microbial suppression, and this research demonstrates the importance of other parameters such as pressure, salinity, heat, and anoxic conditions that will further induce an extreme environment for typical bentonite microbial metabolisms. The data generated by this research suggest some water-activity-dependent microbial selection, and future research will be better informed when testing these conditions alongside other factors of suppression. The results of this study can be compared to previous research including the effects of water activity and salinity on microorganisms in bentonite, with pressure, and can also guide future experimental conditions using pressure in pressure vessel

experiments. The data in this project will contribute to knowledge surrounding DGR specifications needed for microbial suppression and will provide insight into processes that may occur should factors of suppression shift. Research contributing to this field will be used to help guide DGR design specifications to prevent the possibility of microbiologically influenced corrosion of used nuclear fuel containers, and will help to guide a safe and long-term storage solution for used nuclear fuel.

Bibliography

1. Nuclear Waste Management Organization. What is used nuclear fuel? https://www.nwmo.ca/~/media/Site/Files/PDFs/2021/03/15/20/45/Backgrounder-2021-What-is-used-nuclear-fuel.ashx?la=en. Accessed 12 Oct 2021.

2. Nuclear Waste Management Organization. Implementation of adaptive phased management. 2017. Nuclear Waste Management Organization.

3. Nuclear Waste Management Organization. Ensuring safety: Multiple-barrier system. https://www.nwmo.ca/~/media/Site/Files/PDFs/2015/11/16/20/36/Secure_Accessible_MultipleBarrier_Backgrounder_EN.ashx?la=en. Accessed 12 Oct 2021.

4. Nuclear Waste Management Organization. 2020 NWMO annual report. Nuclear Waste Management Organization.

5. Nuclear Waste Management Organization. RD 2019 – NWMO's program for research and development for long-term management of used nuclear fuel. 2019. Nuclear Waste Management Organization.

6. Noronha J. Deep geological repository conceptual design report crystalline/sedimentary rock environment. 2016. Nuclear Waste Management Organization.

7. Cramer JJ. The Cigar Lake uranium deposit: Analog information for Canada's nuclear fuel waste disposal concept. 1995. Atomic Energy of Canada Limited.

8. Badley M, Shoesmith D. The corrosion/dissolution of used nuclear fuel in a deep geological repository. 2022. Nuclear Waste Management Organization, Toronto, ON.

9. Karnland O, Olsson S, Nilsson U. Mineralogy and sealing properties of various bentonites and smectite-rich clay materials. 2006. Swedish Nuclear Fuel and Waste Management Co.

10. Dixon DA. Review of the T-H-M-C properties of MX-80 bentonite. 2019. Nuclear Waste Management Organization.

11. Wang H, Shirakawabe T, Komine H, Ito D, Gotoh T, Ichikawa Y, et al. Movement of water in compacted bentonite and its relation with swelling pressure. *Can Geotech J* 2020; **57**: 921–932.

12. Ballarini E, Graupner B, Bauer S. Thermal–hydraulic–mechanical behavior of bentonite and sand-bentonite materials as seal for a nuclear waste repository: Numerical simulation of column experiments. *Appl Clay Sci* 2017; **135**: 289–299.

13. Stroes-Gascoyne S, Hamon CJ, Maak P, Russell S. The effects of the physical properties of highly compacted smectitic clay (bentonite) on the culturability of indigenous microorganisms. *Appl Clay Sci* 2010; **47**: 155–162.

14. Asad A, Rashwan T, Molnar I, Krol M. Modelling bisulfide transport through the engineered barrier system under repository conditions: Coupling unsaturated flow and refining boundary conditions. 2022. Nuclear Waste Management Organization.

15. King F, Kolar M, Maak P. Reactive-transport model for the prediction of the uniform corrosion behaviour of copper used fuel containers. *J Nucl Mater* 2008; **379**: 133–141.

16. King F, Hall DS, Keech PG. Nature of the near-field environment in a deep geological repository and the implications for the corrosion behaviour of the container. *Corros Eng Sci Technol* 2017; **52**: 25–30.

17. Giroud N, Tomonaga Y, Wersin P, Briggs S, King F, Vogt T, et al. On the fate of oxygen in a spent fuel emplacement drift in Opalinus Clay. *Appl Geochemistry* 2018; **97**: 270–278.

18. Taborowski T, Chukharkina ABA, Blom A, Pedersen K. Bacterial presence and activity in compacted bentonites. 2019. Microbiology in Nuclear Waste Disposal.

19. Bengtsson A, Edlund J, Hallbeck B, Heed C, Pedersen K. Microbial sulphide-producing activity in MX-80 bentonite at 1750 and 2000 kg m^{-3} wet density. 2015. Swedish Nuclear Fuel and Waste Management Co, Stockholm, Sweden.

20. Pedersen K, Motamedi M, Karnland O, Sandén T. Cultivability of microorganisms introduced into a compacted bentonite clay buffer under high-level radioactive repository conditions. *Eng Geol* 2000; **58**: 149–161.

21. Cheng Y, Holman H, Li Z. Remediation of chromium and uranium contamination by microbial activity. *Elements* 2012; **8**: 107–112.

22. Lovley DR, Phillips EJP, Gorby YA, Landa ER. Microbial reduction of uranium. *Nature* 1991; **350**: 413–416.

23. Suzuki Y, Kelly SD, Kemner KM, Banfield JF. Nanometre-size products of uranium bioreduction. *Nature* 2002; **419**: 134.

24. Vachon MA, Engel K, Beaver RC, Slater GF, Binns WJ, Neufeld JD. Fifteen shades of clay: Distinct microbial community profiles obtained from bentonite samples by cultivation and direct nucleic acid extraction. *Sci Rep* 2021; **11**: 22349.

25. Slater GF, Neufeld J, Sherwood Lollar B. Development of microbial characterization techniques for crystalline rock. 2018. Nuclear Waste Management Organization.

26. Chang Y-J, Peacock AD, Long PE, Stephen JR, McKinley JP, Macnaughton SJ, et al. Diversity and characterization of sulfate-reducing bacteria in groundwater at a uranium mill tailings site. *Appl Environ Microbiol* 2001; **67**: 3149–3160.

27. Muyzer G, Stams AJM. The ecology and biotechnology of sulphate-reducing bacteria. *Nat Rev Microbiol* 2008; **6**: 441–454.

28. Pedersen K. Microbial life in deep granitic rock. *FEMS Microbiol Rev* 1997; **20**: 399–414.

29. Pedersen K, Motamedi M, Karnland O. Survival of bacteria in nuclear waste buffer materials. The influence of nutrients, temperature and water activity. 1995. Swedish Nuclear Fuel and Waste Management Co, Stockholm, Sweden.

30. Motamedi M, Karland O, Pedersen K. Survival of sulfate reducing bacteria at different water activities in compacted bentonite. *FEMS Microbiol Lett* 1996; **141**: 83–87.

31. Maanoja S, Lakaniemi A-M, Lehtinen L, Salminen L, Auvinen H, Kokko M, et al. Compacted bentonite as a source of substrates for sulfate-reducing microorganisms in a simulated excavation-damaged zone of a spent nuclear fuel repository. *Appl Clay Sci* 2020; **196**: 105746.

32. Suckling P, Avis J, Calder N, Nasir O, Humphreys P, King F, et al. Gas generation and transport code. 2015. Nuclear Waste Management Organization.

33. Plugge C, Zhang W, Scholten J, Stams A. Metabolic flexibility of sulfate-reducing bacteria. *Front Microbiol* 2011; **2**.

34. Ozuolmez D, Na H, Lever M, Kjeldsen K, Jørgensen B, Plugge C. Methanogenic archaea and sulfate reducing bacteria co-cultured on acetate: teamwork or coexistence? *Front Microbiol* 2015; **6**: 492.

35. Masurat P, Eriksson S, Pedersen K. Evidence of indigenous sulphate-reducing bacteria in commercial Wyoming bentonite MX-80. *Appl Clay Sci* 2010; **47**: 51–57.

36. Briggs S, McKelvie J, Sleep B, Krol M. Multi-dimensional transport modelling of corrosive agents through a bentonite buffer in a Canadian deep geological repository. *Sci Total Environ* 2017; **599–600**: 348–354.

37. Little B, Wagner P, Mansfeld F. An overview of microbiologically influenced corrosion. *Electrochim Acta* 1992; **37**: 2185–2194.

38. King F. Microbiologically influenced corrosion of nuclear waste containers. *Corrosion* 2009; **65**: 233–251.

39. Jalique DR, Stroes-Gascoyne S, Hamon CJ, Priyanto DG, Kohle C, Evenden WG, et al. Culturability and diversity of microorganisms recovered from an eight-year old highly-compacted, saturated MX-80 Wyoming bentonite plug. *Appl Clay Sci* 2016; **126**: 245–250.

40. Gilmour KA, Davie CT, Gray N. Survival and activity of an indigenous iron-reducing microbial community from MX80 bentonite in high temperature / low water environments with relevance to a proposed method of nuclear waste disposal. *Sci Total Environ* 2022; **814**: 152660.

41. Pedersen K. Microbial processes in radioactive waste disposal. 2000. Swedish Nuclear Fuel and Waste Management Co, Stockholm, Sweden.

42. Ruiz-Fresneda MA, Martinez-Moreno MF, Povedano-Priego C, Morales-Hidalgo M, Jroundi F, Merroun ML. Impact of microbial processes on the safety of deep geological repositories for radioactive waste. *Front Microbiol* 2023; **14**: 1134078.

43. Stevens TO, McKinley JP. Lithoautotrophic microbial ecosystems in deep basalt aquifers. *Science* 1995; **270**: 450–455.

44. Mijnendonckx K, Miroslav H, Wang L, Jacops E, Provoost A, Mysara M, et al. An active microbial community in Boom Clay pore water collected from piezometers impedes validating predictive modelling of ongoing geochemical processes. *Appl Geochemistry* 2019; **106**: 149–160.

45. Povedano-Priego C, Jroundi F, Lopez-Fernandez M, Shrestha R, Spanek R, Martín-Sánchez I, et al. Deciphering indigenous bacteria in compacted bentonite through a novel and efficient DNA extraction method: Insights into biogeochemical processes within the Deep Geological Disposal of nuclear waste concept. *J Hazard Mater* 2021; **408**: 124600.

46. Bagnoud A, Leupin O, Schwyn B, Bernier-Latmani R. Rates of microbial hydrogen oxidation and sulfate reduction in Opalinus Clay rock. *Appl Geochemistry* 2016; **72**: 42–50.

47. Beaton D, Stuart M, Neal P. Influence of microbial degradation on gas pressure evolution and terminal gas composition in batch anaerobic containers of surrogate low-to-intermediate level radioactive waste. 2018. Canadian Nuclear Laboratories.

48. Schultz C. Water activity as related to microorganisms in the manufacturing environment. *Gen Int Med Clin Innov* 2016; **1**: 1–2.

49. Stroes-Gascoyne S, Hamon CJ, Dixon DA, Martino JB. Microbial analysis of samples from the tunnel sealing experiment at AECL's Underground Research Laboratory. *Phys Chem Earth* 2007; **32**: 219–231.

50. Stevenson A, Cray JA, Williams JP, Santos R, Sahay R, Neuenkirchen N, et al. Is there a common water-activity limit for the three domains of life? *ISME J* 2015; **9**: 1333–1351.

51. Fu Z, Wang H, Li J, Lu Y. Determination of moisture content and shrinkage strain during wood water loss with electrochemical method. *Polymers (Basel)* 2022; **14**: 778.

52. Villar MV, Lloret A. Influence of dry density and water content on the swelling of a compacted bentonite. *Appl Clay Sci* 2008; **39**: 38–49.

53. Stroes-Gascoyne S, Haveman SA, Hamon CJ, Delaney T-L, Pedersen K, Arlinger J, et al. Occurrence and identification of microorganisms in compacted clay-based buffer material designed for use in a nuclear fuel waste disposal vault. *Can J Microbiol* 1997; **43**: 1133–1146.

54. Hedin A. Long-term safety for KBS-3 repositories at Forsmark and Laxemar – a first evaluation. 2006. Swedish Nuclear Fuel and Waste Management Co, Stockholm, Sweden.

55. Asensio L, De la Morena G, López-Vizcaíno R, Yustres Á, Navarro V. Salinity effects on the erosion behaviour of MX-80 bentonite: A modelling approach. *Appl Clay Sci* 2018; **161**: 494–504.

56. Alawaji HA. Swell and compressibility characteristics of sand–bentonite mixtures inundated with liquids. *Appl Clay Sci* 1999; **15**: 411–430.

57. Bengtsson A, Pedersen K. Microbial sulphate-reducing activity over load pressure and density in water saturated Boom Clay. *Appl Clay Sci* 2016; **132–133**: 542–551.

58. Stroes-Gascoyne S, Hamon CJ. The role of highly compacted bentonite in localized suppression of microbial activity in a nuclear fuel waste repository. 2011. Canadian Nuclear Society, Toronto, ON.

59. Hillmer N, Bothwell R. Geography of Ontario. *The Canadian Encyclopedia*. 2023. Historica Canada.

60. Behazin M, Pedersen K, Long L, Abrahamsen-Mills L, Boylan A, Bryan N. State of science review of sulfide production in deep geological repositories for used nuclear fuel. 2021. Nuclear Waste Management Organization.

61. Radakovic-Guzina Z, Riahi A, Damjanac B. Long-term stability analysis of APM conceptual repository design in sedimentary and crystalline rock settings. 2015. Nuclear Waste Management Organization.

62. Nuclear Waste Management Organization. Postclosure safety assessment of a used fuel repository in crystalline rock. 2017. Nuclear Waste Management Organization.

63. Nuclear Waste Management Organization. Postclosure safety assessment of a used fuel repository in sedimentary rock. 2018. Nuclear Waste Management Organization.

64. Gobien M, Garisto F, Kremer E, Medri C. Seventh case study: Reference data and codes. 2018. Nuclear Waste Management Organization.

65. Stroes-Gascoyne S, Hamon CJ, Maak P. Limits to the use of highly compacted bentonite as a deterrent for microbiologically influenced corrosion in a nuclear fuel waste repository. *Phys Chem Earth* 2011; **36**: 1630–1638.

66. Beaver RC, Engel K, Binns WJ, Neufeld JD. Microbiology of barrier component analogues of a deep geological repository. *Can J Microbiol* 2022; **68**: 73–90.

67. Marshall KC. Clay mineralogy in relation to survival of soil bacteria. *Annu Rev Phytopathol* 1975; **13**: 357–373.

68. Onstott TC, Phelps TJ, Colwell FS, Ringelberg D, White DC, Boone DR, et al. Observations pertaining to the origin and ecology of microorganisms recovered from the deep subsurface of Taylorsville Basin, Virginia. *Geomicrobiol J* 1998; **15**: 353–385.

69. Acinas SG, Marcelino LA, Klepac-Ceraj V, Polz MF. Divergence and redundancy of 16S rRNA sequences in genomes with multiple rrn operons. *J Bacteriol* 2004; **186**: 2629–2635.

70. Crosby LD, Criddle CS. Understanding bias in microbial community analysis techniques due to rrn operon copy number heterogeneity. *Biotechniques* 2003; **34**: 790–802.

71. Engel K, Coyotzi S, Vachon MA, McKelvie JR, Neufeld JD. Validating DNA extraction protocols for bentonite clay. *mSphere* 2019; **4**: e00334-19.

72. Beall GW, Sowersby DS, Roberts RD, Robson MH, Lewis LK. Analysis of oligonucleotide DNA binding and sedimentation properties of montmorillonite clay using ultraviolet light spectroscopy. *Biomacromolecules* 2009; **10**: 105–112.

73. Engel K, Ford SE, Coyotzi S, McKelvie J, Diomidis N, Slater G, et al. Stability of microbial community profiles associated with compacted bentonite from the Grimsel Underground Research Laboratory. *mSphere* 2019; **4**: e00601-19.

74. Stroes-Gascoyne S, Schippers A, Schwyn B, Poulain S, Sergeant C, Simonoff M, et al. Microbial community analysis of Opalinus clay drill core samples from the Mont Terri underground research laboratory, Switzerland. *Geomicrobiol J* 2007; **24**: 1–17.

75. Engel K, Coyotzi S, Slater G, Neufeld J. Development of protocols for sampling and assessment of bentonite and environmental samples associated with in situ proof tests of engineered barrier systems. 2018. Nuclear Waste Management Organization, Toronto, ON.

76. White DC, Ringelberg DB. Utility of the signature lipid biomarker analysis in determining the in situ viable biomass, community structure, and nutritional/physiologic status of deep subsurface microbiota. *Microbiology of the Terrestrial Deep Subsurface*. 1997. CRC Press.

77. Burzan N, Murad Lima R, Frutschi M, Janowczyk A, Reddy B, Rance A, et al. Growth and persistence of an aerobic microbial community in Wyoming bentonite MX-80 despite anoxic in situ conditions. *Front Microbiol* 2022; **13**: 858324.

78. Svensson D, Kalinowski B, Turner S, Dopson M. Activity of sulphate reducing bacteria in bentonite as a function of water availability. 2020. Swedish Nuclear Fuel and Waste Management Co, Sweden.

79. Usman MO, Simpson MJ. Assessment of the molecular-level compositional heterogeneity of natural organic matter in bentonites intended for long-term used nuclear fuel storage. *Org Geochem* 2021; **152**: 104166.

80. Blodgett R. BAM Appendix 2: Most probable number from serial dilutions. *U.S. Food & Drug Administration*. https://www.fda.gov/food/laboratory-methods-food/bam-appendix-2-most-probable-number-serial-dilutions.

81. Muyzer G, de Waal EC, Uitterlinden AG. Profiling of complex microbial populations by denaturing gradient gel electrophoresis analysis of polymerase chain reaction-amplified genes coding for 16S rRNA. *Appl Environ Microbiol* 1993; **59**: 695–700.

82. Parada AE, Needham DM, Fuhrman JA. Every base matters: assessing small subunit rRNA primers for marine microbiomes with mock communities, time series and global field samples. *Environ Microbiol* 2016; **18**: 1403–1414.

83. Quince C, Lanzen A, Davenport RJ, Turnbaugh PJ. Removing noise from pyrosequenced amplicons. *BMC Bioinform* 2011; **12**: 38.

84. Bartram AK, Lynch MDJ, Stearns JC, Moreno-Hagelsieb G, Neufeld JD. Generation of multimillion-sequence 16S rRNA gene libraries from complex microbial communities by assembling paired-end illumina reads. *Appl Environ Microbiol* 2011; **77**: 3846–3852.

85. Bolyen E, Rideout JR, Dillon MR, Bokulich NA, Abnet CC, Al-Ghalith GA, et al. Reproducible, interactive, scalable and extensible microbiome data science using QIIME 2. *Nat Biotechnol* 2019; **37**: 852–858.

86. Min D, Doxey AC, Neufeld JD. AXIOME3: Automation, eXtension, and Integration Of Microbial Ecology. *GigaScience* 2021; **10**: giab006.

87. Callahan BJ, McMurdie PJ, Rosen MJ, Han AW, Johnson AJA, Holmes SP. DADA2: High-resolution sample inference from Illumina amplicon data. *Nat Methods* 2016; **13**: 581–583.

88. Pruesse E, Quast C, Knittel K, Fuchs BM, Ludwig W, Peplies J, et al. SILVA: a comprehensive online resource for quality checked and aligned ribosomal RNA sequence data compatible with ARB. *Nucleic Acids Res* 2007; **35**: 7188–7196.

89. Davis NM, Proctor DM, Holmes SP, Relman DA, Callahan BJ. Simple statistical identification and removal of contaminant sequences in marker-gene and metagenomics data. *Microbiome* 2018; **6**: 226.

90. R Core Team. R: A language and environment for statistical computing. 2023. R Foundation for Statistical Computing, Vienna, Austria.

91. De Cáceres M, Legendre P. Associations between species and groups of sites: indices and statistical inference. *Ecol* 2009; **90**: 3566–3574.

92. De Cáceres M, Legendre P, Moretti M. Improving indicator species analysis by combining groups of sites. *Oikos* 2010; **119**: 1674–1684.

93. Caporaso JG, Lauber CL, Walters WA, Berg-Lyons D, Lozupone CA, Turnbaugh PJ, et al. Global patterns of 16S rRNA diversity at a depth of millions of sequences per sample. *Proc Natl Acad Sci* 2011; **108**: 4516–4522.

94. Liu CM, Kachur S, Dwan MG, Abraham AG, Aziz M, Hsueh P-R, et al. FungiQuant: A broad-coverage fungal quantitative real-time PCR assay. *BMC Microbiol* 2012; **12**: 255.

95. Pedersen K, Ekendahl S. Distribution and activity of bacteria in deep granitic groundwaters of southeastern Sweden. *Microb Ecol* 1990; **20**: 37–52.

96. Wu WJ, Chang J. Effect of oxygen on the germination and culturability of *Bacillus atrophaeus* spores. *Int Microbiol* 2022; **25**: 353–363.

97. Matschiavelli N, Kluge S, Podlech C, Standhaft D, Grathoff G, Ikeda-Ohno A, et al. The year-long development of microorganisms in uncompacted Bavarian bentonite slurries at 30 and 60 °C. *Environ Sci Technol* 2019; **53**: 10514–10524.

98. Wang Y, Shi J, Tang L, Zhang Y, Zhang Y, Wang X, et al. Evaluation of Rpf protein of *Micrococcus luteus* for cultivation of soil actinobacteria. *Syst Appl Microbiol* 2021; **44**: 126234.

99. Locey KJ, Lennon JT. Scaling laws predict global microbial diversity. *Proc Natl Acad Sci* 2016; **113**: 5970–5975.

100. Zhao K, Li J, Shen M, Chen Q, Liu M, Ao X, et al. Actinobacteria associated with Chinaberry tree are diverse and show antimicrobial activity. *Sci Rep* 2018; **8**: 11103.

101. Bodor A, Bounedjoum N, Vincze GE, Erdeiné Kis Á, Laczi K, Bende G, et al. Challenges of unculturable bacteria: Environmental perspectives. *Rev Environ Sci Biotechnol* 2020; **19**: 1–22.

102. Carini P, Marsden PJ, Leff JW, Morgan EE, Strickland MS, Fierer N. Relic DNA is abundant in soil and obscures estimates of soil microbial diversity. *Nat Microbiol* 2016; **2**: 16242.

103. Lennon JT, Muscarella ME, Placella SA, Lehmkuhl BK. How, when, and where relic DNA affects microbial diversity. *mBio* 2018; **9**: e00637-18.

104. Gustave W, Yuan Z-F, Sekar R, Toppin V, Liu J-Y, Ren Y-X, et al. Relic DNA does not obscure the microbial community of paddy soil microbial fuel cells. *Res Microbiol* 2019; **170**: 97–104.

105. Nguyen LT, Zajíčková M, Mašátová E, Matoušková P, Skálová L. The ATP bioluminescence assay: a new application and optimization for viability testing in the parasitic nematode *Haemonchus contortus*. *Vet Res* 2021; **52**: 124.

106. Suszynski TM, Wildey GM, Falde EJ, Cline GW, Maynard KS, Ko N, et al. The ATP/DNA ratio is a better indicator of islet cell viability than the ADP/ATP ratio. *Transplant Proc* 2008; **40**: 346–350.

107. Eydal HSC, Pedersen K. Use of an ATP assay to determine viable microbial biomass in Fennoscandian Shield groundwater from depths of 3–1000 m. *J Microbiol Methods* 2007; **70**: 363–373.

108. Lydmark S, Pedersen K. Äspö Hard Rock Laboratory. Canister Retrieval Test. Microorganisms in buffer from the Canister Retrieval Test – numbers and metabolic diversity. 2011. Swedish Nuclear Fuel and Waste Management Co.

109. Hlavackova V, Shrestha R, Hofmanova E, Kejzlar P, Riha J, Bartak D, et al. A protocol for the extraction of viable bacteria for identification of bacterial communities in bentonite. *Appl Clay Sci* 2023; **232**: 106809.

110. Kobayashi H, Oethinger M, Tuohy MJ, Hall GS, Bauer TW. Improving clinical significance of PCR: use of propidium monoazide to distinguish viable from dead *Staphylococcus aureus* and *Staphylococcus epidermidis*. *J Orthop Res* 2009; **27**: 1243–1247.

111. Zi C, Zeng D, Ling N, Dai J, Xue F, Jiang Y, et al. An improved assay for rapid detection of viable *Staphylococcus aureus* cells by incorporating surfactant and PMA treatments in qPCR. *BMC Microbiol* 2018; **18**: 132.

112. Karstens L, Asquith M, Davin S, Fair D, Gregory WT, Wolfe AJ, et al. Controlling for contaminants in low-biomass 16S rRNA gene sequencing experiments. *mSystems* 2019; **4**: e00290-19.

113. Glassing A, Dowd SE, Galandiuk S, Davis B, Chiodini RJ. Inherent bacterial DNA contamination of extraction and sequencing reagents may affect interpretation of microbiota in low bacterial biomass samples. *Gut Pathog* 2016; **8**: 24.

114. van Bergeijk DA, Terlouw BR, Medema MH, van Wezel GP. Ecology and genomics of Actinobacteria: New concepts for natural product discovery. *Nat Rev Microbiol* 2020; **18**: 546–558.

115. Sayed AM, Abdel-Wahab NM, Hassan HM, Abdelmohsen UR. *Saccharopolyspora*: An underexplored source for bioactive natural products. *J Appl Microbiol* 2020; **128**: 314–329.

116. Matschiavelli M, Steglich J, Kluge S, Cherkouk C. Bentonite - Geotechnical barrier and source for microbial life. 2016. International Atomic Energy Agency.

117. Ševců A, Steinová J, Burkartová K, Černá K. Microbial diversity in aged bentonites. 2018. Microbiology in Nuclear Waste Disposal.

118. Gilmour KA, Davie CT, Gray N. An indigenous iron-reducing microbial community from MX80 bentonite - A study in the framework of nuclear waste disposal. *Appl Clay Sci* 2021; **205**: 106039.

119. Chater KF. *Streptomyces* inside-out: A new perspective on the bacteria that provide us with antibiotics. *Philos Trans R Soc Lond B Biol Sci* 2006; **361**: 761–768.

120. Bennett JA, Kandell GV, Kirk SG, McCormick JR. Visual and microscopic evaluation of *Streptomyces* developmental mutants. *J Vis Exp* 2018; **139**: 57373.

121. Chander Y, Kumar K, Goyal SM, Gupta SC. Antibacterial activity of soil-bound antibiotics. *J Environ Qual* 2005; **34**: 1952–1957.

122. Kümmerer K. Antibiotics in the aquatic environment – A review – Part I. *Chemosphere* 2009; **75**: 417–434.

123. Cycoń M, Mrozik A, Piotrowska-Seget Z. Antibiotics in the soil environment—Degradation and their impact on microbial activity and diversity. *Front Microbiol* 2019; **10**: 338.

124. Cheng R, Wang X, Zhu H, Yan B, Shutes B, Xu Y, et al. Isolation and characterization of a salt-tolerant denitrifying bacterium *Alishewanella* sp. F2 from seawall muddy water. *Sci Rep* 2020; **10**: 10002.

125. Hirose S, Tank M, Hara E, Tamaki H, Mori K, Takaichi S, et al. *Aquabacterium pictum* sp. nov., the first aerobic bacteriochlorophyll a-containing fresh water bacterium in the genus *Aquabacterium* of the class *Betaproteobacteria*. *Evol Microbiol* 2020; **70**: 596–603.

126. Leys NMEJ, Ryngaert A, Bastiaens L, Verstraete W, Top EM, Springael D. Occurrence and phylogenetic diversity of *Sphingomonas* strains in soils contaminated with polycyclic aromatic hydrocarbons. *Appl Environ Microbiol* 2004; **70**: 1944–1955.

127. Willems A. The Family Comamonadaceae. In: Rosenberg E, DeLong EF, Lory S, Stackebrandt E, Thompson F (eds). *The Prokaryotes: Alphaproteobacteria and Betaproteobacteria*. 2014. Springer, Berlin, Heidelberg, pp 777–851.

128. Povedano-Priego C, Jroundi F, Lopez-Fernandez M, Morales-Hidalgo M, Martin-Sánchez I, Huertas FJ, et al. Impact of anoxic conditions, uranium (VI) and organic phosphate substrate on the biogeochemical potential of the indigenous bacterial community of bentonite. *Appl Clay Sci* 2022; **216**: 106331.

129. Yuan L-J, Zhang Y-Q, Guan Y, Wei Y-Z, Li Q-P, Yu L-Y, et al. *Saccharopolyspora antimicrobica* sp. nov., an actinomycete from soil. *Int J Syst Evol Microbiol* 2008; **58**: 1180–1185.

130. Lv L-L, Zhang Y-F, Xia Z-F, Zhang J-J, Zhang L-L. *Saccharopolyspora halotolerans* sp. nov., a halophilic actinomycete isolated from a hypersaline lake. *Int J Syst Evol Microbiol* 2014; **64**: 3532–3537.

131. Meklat A, Bouras N, Zitouni A, Sabaou N, Mathieu F, Schumann P, et al. *Saccharopolyspora ghardaiensis* sp. nov., an extremely halophilic actinomycete isolated from Algerian Saharan soil. *J Antibiot* 2014; **67**: 299–303.

132. Asquith E, Evans C, Dunstan RH, Geary P, Cole B. Distribution, abundance and activity of geosmin and 2-methylisoborneol-producing *Streptomyces* in drinking water reservoirs. *Water Res* 2018; **145**: 30–38.

133. Cochet N, Demain AL. Effect of water activity on production of β-lactam antibiotics by *Streptomyces clavuligerus* in submerged culture. *J Appl Bacteriol* 1996; **80**: 333–337.

134. Chi Fru E, Athar R. In situ bacterial colonization of compacted bentonite under deep geological high-level radioactive waste repository conditions. *Appl Microbiol Biotechnol* 2008; **79**: 499–510.

135. Ranjani A, Dhanasekaran D, Gopinath PM. An introduction to Actinobacteria. In: Dhanasekaran D, Jiang Y (eds). *Actinobacteria - Basics and biotechnological applications*. 2016. InTech.

136. Drake H, Ivarsson M, Bengtson S, Heim C, Siljeström S, Whitehouse MJ, et al. Anaerobic consortia of fungi and sulfate reducing bacteria in deep granite fractures. *Nat Commun* 2017; **8**: 55.